EFFECT OF CHEMICAL TREATMENT ON III-NITRIDE SURFACE CHARACTERISTICS

By

KANG-NYUNG LEE

A DISSERTATION PRESENTED TO THE GRADUATE SCHOOL
OF THE UNIVERSITY OF FLORIDA IN PARTIAL FULFILLMENT
OF THE REQUIREMENTS FOR THE DEGREE OF
DOCTOR OF PHILOSOPHY

UNIVERSITY OF FLORIDA

2000

Copyright 2000

by

KANG-NYUNG LEE

DEDICATED TO MY WIFE AND FAMILY

ACKNOWLEDGMENTS

The biggest thanks go to my adviser, Dr. Cammy Abernathy who has given me great support with knowledge as well as encouragement. I also deeply appreciate Dr. Stephen Pearton, Dr. Stanley Bates, Dr. Rajiv Singh and Dr. Fred Sharifi for spending their precious time as committee members.

I acknowledge the support of Brent Gila, Mark Overberg and the staff at Microfabritech facility.

TABLE OF CONTENTS

page

ACKNOWLEDGMENTS....iv

LIST OF TABLES....vi

LIST OF FIGURES....vii

ABSTRACT....xi

CHAPTERS

1 INTRODUCTION/BACKGROUND....1
  1.1 III-Nitride Semiconductors/Devices....1
  1.2 Importance of Surface States....3
  1.3 Review of Surface Chemical Treatments....8
  1.4 Technical Rationale/Objective of this Study....11

2 EXPERIMENTAL PROCEDURES....15

3 SURFACE CLEANING OF AlN....18

4 SURFACE CLEANING OF GaN....27
  4.1 Ex-situ Cleaning....28
  4.2 In-situ Cleaning....30
    4.2.1. Thermal/Plasma Cleaning....30
    4.2.2. Chemical Beam (PCl_3, TDMAP) Cleaning....33
  4.3 Electrical Characteristics....37

5 GENERATION AND REMOVAL OF THERMAL DAMAGE....67

6 SUMMARY....86

LIST OF REFERENCES....88

BIOGRAPHICAL SKETCH....93

LIST OF TABLES

Table page

1-1. Relative bond strengths of constituents commonly found in MBE, MOCVD and MOMBE growth....4

3-1. AES peak-to-peak height ratios for the UV/O_3 and various wet chemically treated AlN surfaces....25

4-1. AES peak-to-peak height ratios for the UV/O_3 and various wet chemically treated GaN surfaces....44

4-2. Comparison of surface atomic concentration of C and O between AES and SIMS analysis on GaN after various combination of wet chemical and thermal surface treatment....51

4-3. Atomic concentration of interfacial impurities as measured by SIMS after various chemical treatments on the GaN before AlN deposition....66

5-1. Summary of characteristics of n-GaN Schottky diodes....76

LIST OF FIGURES

Figure page

1-1. Schematic energy-band diagram of an MIS structure, illustrating the presence of surface states....5

3-1. AES survey spectra of AlN (a) as-received, (b) PR deposit/strip, (c) acid cleaned for 3 min in 1:1 HF:DI, and (d) acid cleaned and 50-min UV/O_3 exposure....22

3-2. Surface atomic concentration of carbon and oxygen on AlN surface after various wet chemical treatments....23

3-3. AFM images and RMS roughness values of AlN surfaces after various wet chemical treatments (a) as-received, (b) solvents (acetone/methanol, each 5 min), (c) 1:1 HF:DI, 3 min and (d) 1:1 HF:DI, 3 min and UV/O_3, 25 min....24

3-4. Surface atomic concentration of oxygen and carbon as measured by AES on AlN after various combinations of wet chemical and thermal surface treatment. All samples were exposed to photoresist (PR) which was followed by the HF/O_3 procedure before treatment....26

4-1. AES survey spectra of GaN (a) as-received, (b) PR deposit/strip, (c) acid cleaned for 3 min in 1:1 HCl:DI, (d) acid cleaned with 25-min UV/O_3 and (e) PR deposit/strip, acid cleaned and 25 min UV/O_3....43

4-2. AFM images and RMS roughness values of GaN surfaces after various wet chemical treatments (a) as-received, (b) solvents (acetone/methanol, each 5 min), (c) 1:1 HCl:DI, 3 min and (d) 1:1 HCl:DI, 3 min and UV/O_3, 25 min....45

4-3. RHEED patterns taken along the [11-20] azimuth on the MOCVD-grown GaN surfaces after various chemical treatments (a) as-received GaN (b) HCl/O_3/HF-treated GaN and (c) HCl/O_3/AZ 400K-treated GaN....46

4-4. Surface atomic concentration of oxygen and carbon as measured by AES on GaN after various combinations of wet chemical and thermal surface treatment. All samples were exposed to PR which was followed by the HCl /O_3 cleaning procedure before treatment....47

4-5. AFM images and RMS roughness values for regrown GaN capping layers on (a) as-received, (b) 5 sccm N_2 plasma exposure at 750°C for 5 min, (c) 5 sccm N_2 plasma exposure at 900°C for 5 min, (d) the mixture of 7.5 sccm H_2 and 2 sccm N_2 plasma exposure at 750°C for 5 min The (b), (c), and (d) samples were exposed to PR, 1:1 HCl:DI, 3 min, and 25 min UV/O_3 before in-situ treatment............................48

4-6. Surface atomic concentration of carbon and oxygen as measured by AES on GaN after H_2/N_2 plasma exposure at different temperatures. All samples were treated with PR/HCl/O_3 prior to plasma exposure..49

4-7. SEM images of GaN surfaces (15 kV, x10,000) (a) as-received MOCVD-grown GaN substrate and (b), (c) and (d) are MBE-regrown GaN on MOCVD-grown GaN substrate after exposure to H_2/N_2 plasma for 10 min. at 500°C, 650°C and 750°C, respectively..50

4-8. RHEED patterns taken along the [11-20] azimuth on the MOCVD-grown GaN surfaces after various chemical and thermal treatments (a) HCl/O_3/HF treated GaN, (b) HCl/O_3/AZ 400K treated GaN, (c) HCl/O_3/HF treatment followed by thermal annealing at 700°C and (d) HCl/O_3/AZ 400K followed by thermal annealing at 700°C..52

4-9. SIMS depth profiles of carbon and oxygen impurities for the MBE-regrown GaN layers on MOCVD-grown GaN substrates (a) overgrowth only at 500°C without N_2 plasma exposure, (b) overgrowth only at 650°C with N_2 plasma exposure during substrate heating to growth temperature (c) PCl_3 exposure at 500°C for 10 min. and (d) TDMAP exposure at 500°C for 10 min. without N_2 plasma exposure before regrowth...53, 54

4-10. Tapping mode AFM images of the as-received MOCVD-grown GaN substrate. The RMS roughness value of this sample is 1.8 nm...................................55

4-11. AFM images of the MBE-grown GaN layers on MOCVD grown GaN substrates (a) overgrowth only at 500°C without N_2 plasma exposure, (b) overgrowth only at 650°C without N_2 plasma exposure and (c) overgrowth only with N_2 plasma exposure during substrate heating to growth temperatures. The RMS roughness values of (a), (b) and (c) are 15.5, 7.6 and 2.0 nm, respectively.......................56

4-12. AFM images of regrown MBE GaN on MOCVD-grown GaN substrates after (a) TDMAP exposure at 500°C without N_2 plasma and (b) with N_2 plasma during substrate heating to growth temperature and TDMAP exposure. The RMS roughness values of (a) and (b) are 1.35 and 2.17 nm, respectively.................57

4-13. AFM images of regrown MBE GaN on MOCVD-grown GaN substrates after (a) PCl_3 exposure at 500°C for 10 min without N_2 plasma and (b) PCl_3 exposure at 650°C for 10 min with N_2 plasma exposure during substrate heating and PCl_3 exposure. The RMS roughness values of (a) and (b) are 4.36 and 9.6 nm...........58

4-14. AlN/GaN MIS diode structure……59

4-15. I-V characteristics from the AlN/GaN MIS diodes after surface pretreatment before growth of AlN layers……60

4-16. I-V characteristics from the AlN/GaN MIS diodes after in-situ surface chemical treatments before the AlN layer growth. The HCl/O_3 cleaning procedure was applied for all samples before in-situ treatment……61

4-17. AFM images of (a) as-received MOCVD GaN, (b) AlN grown on MOCVD GaN after N_2 plasma exposure at 650°C for 10 min, (c) after PCl_3 exposure at 500°C for 5 min and (d) after TDMAP exposure at 500°C for 5 min of GaN before AlN growth. 1:1 $HCl:H_2O$ and UV/O_3 cleaning were performed before thermal treatments for (b), (c) and (d) samples. The RMS roughness values of (a), (b), (c) and (d) are 1.83, 1.52, 1.55 and 1.09 nm, respectively……62

4-18. AFM images of (a) as-received MOCVD GaN, (b) AlN grown on MOCVD GaN after $HCl/O_3/HF$ followed by thermal annealing at 700°C, (c) after PCl_3 exposure at 300°C, (d) after PCl_3 exposure at 400°C, (e) after PCl_3 exposure at 500°C and (f) after PCl_3 exposure at 600°C. For (c), (d), (e) and (f) samples, HCl/O_3 treatment was performed before PCl_3 exposure. The RMS roughness values of (a), (b), (c), (d), (e), (f) are 0.87, 2.60, 2.81, 2.62, 2.57, 4.45 nm, respectively……63

4-19. I-V characteristics from the AlN/GaN MIS diodes fabricated from samples from treated with various chemical procedures prior to AlN deposition……64

4-20. AFM (left) and RHEED (right) images of the MOCVD GaN (a) as-received, (b) after PCl_3 exposure at 300°C and (c) after PCl_3 exposure at 500°C. The RMS roughness values of (a), (b) and (c) are 0.72, 0.76 and 0.94 nm, respectively. RHEED patterns were taken along the [11-20] azimuth……65

5-1. Layer sructures of the planar Schottky diodes (a) n-GaN Schottky diode and (b) p-GaN Schottky diode……74

5-2. I-V characteristics from the n-GaN Schottky diodes formed after annealing at different temperatures……75

5-3. SEM images of the n-GaN surface (a) after annealing at 400°C, (b) after annealing at 900°C, (c) after annealing at 400°C followed by ozone/HCl treatment and (d) after annealing at 900°C followed by ozone/HCl treatment……77

5-4. I-V characteristics from the n-GaN Schottky diodes after annealing and ozone/HCl treatment……78

5-5. AFM images of n-GaN surface after annealing and ozone/HCl treatment……79

5-6. Annealing temperature dependence of the reverse I-V characteristics of the p-GaN Schottky diodes..80

5-7. High current I-V characteristics from the p-GaN Schottky diodes after annealing and ozone/HCl treatment...81

5-8. Low current I-V characteristics from the p-GaN Schottky diodes after annealing and ozone/HCl treatment...82

5-9. I-V characteristics from n-GaN Schottky diodes annealed at 900°C or annealed at 900°C and then O_3/HCl procedures followed by N_2 plasma or PCl_3 exposure........83

5-10. I-V characteristics from n-GaN Schottky diodes annealed at 900°C or annealed at 900°C and then O_3/HCl procedures followed by N_2 plasma or PCl_3 exposure to remove thermally damaged layers...84

5-11. SEM images of n-GaN surface for annealed at 900°C followed by (a) N_2 plasma exposure at 750°C for 10 min, (b) O_3/HCl procedures and then N_2 plasma exposure at 750°C for 10 min, (c) PCl_3 exposure at 550°C for 10 min, and (d) O_3/HCl procedure and then PCl_3 exposure at 550°C for 10 min...............................85

Abstract of Dissertation Presented to the Graduate School
of the University of Florida in Partial Fulfillment of the
Requirements for the Degree of Doctor of Philosophy

EFFECT OF CHEMICAL TREATMENT ON III-NITRIDE SURFACE CHARACTERISTICS

By

Kang-Nyung Lee

August, 2000

Chairman: Cammy R. Abernathy
Major Department: Materials Science and Engineering

Surface cleaning has a significant influence on the overall performance and reliability of semiconductor devices. III-nitride device technology, like other advanced semiconductor device technologies, most likely will require multiple processing/regrowth steps and several photolithography / dry etching steps to define active device areas. The surface used for epitaxial regrowth, deposition of gate dielectrics, or Ohmic/Schottky metal deposition must be clean and smooth for the fabrication of high quality electronic and photonic devices. This surface cleaning will include the removal of native oxides, organic contaminants, metallic impurities, particulates and chemical residuals.

In this study, various surface-cleaning techniques for the removal of carbon (C) and oxygen (O) from AlN and GaN were investigated. The utility of various cleaning techniques was assessed by chemical, structural and electrical characterization. Auger electron spectroscopy (AES) analysis showed that ex-situ UV/O_3 and wet chemical treatments based on HF and HCl were very effective in removing surface C and reducing the native oxide on both AlN and GaN. After H_2 and N_2 plasma treatments in ultra high vacuum (UHV) at temperatures of 750°C and 900°C, clean GaN surfaces could be achieved within the detection limits of AES. However, secondary ion mass spectroscopy (SIMS) analysis showed that significant concentrations of surface C and O still exist on plasma treated GaN. Further in-situ cleaning methods were performed to obtain clean GaN and AlN surfaces using chemical beam-etching techniques at various temperatures. SIMS and current-voltage (I-V) results showed that PCl_3 chemical beam treatment at 500°C on GaN surface was the most successful in removing the interfacial oxide. This removal of the surface oxide from the GaN substrate may improve the quality of the regrown GaN and allow better quality growth of AlN gate dielectrics.

Also, the effect of annealing on the behavior of GaN Schottky diodes was investigated. Rapid thermal annealing experiments were performed in N_2 ambients for 30 sec at temperatures of 500 to 1000°C. Only annealing at temperatures ≥ 900°C significantly degraded the Schottky diode characteristics. This degradation is believed to be due to the preferential loss of surface nitrogen. Ozone/HCl surface chemical treatments were only partially successful in repairing the thermal damage. The sample exposed to N_2 plasma at 750°C after being thermally damaged showed the worst Schottky diode characteristics due to the highly increased surface nitrogen vacancies, while PCl_3 exposure removed the thermally damaged surface.

CHAPTER 1
INTRODUCTION/BACKGROUND

1.1 III-Nitride Semiconductors/Devices

III-nitrides have received a great deal of attention during the last several years because of their excellent potential as materials for optoelectronic devices in the blue to ultraviolet range.[1] The wurtzite polytypes of GaN, AlN and InN form a wide range of ternary (AlGaN, InGaN, InAlN) and quaternary (InGaAlN) alloy compositions whose direct bandgaps range from 1.9eV for InN, to 3.4eV for GaN, to 6.2eV for AlN. These alloys have application to blue/UV light emitting diodes, laser diodes and UV detectors. Recent developments of III-nitrides have extended their applications greatly in the areas of electrical devices as well as in the areas of optical devices. In particular III-nitrides have significant advantages for high-temperature and high-power device applications because of their wide bandgaps, high breakdown fields, high electron saturation velocities and good thermal stability.[2]

High-temperature devices are defined as those which can operate at temperatures in excess of 300°C. High-temperature semiconductor devices would provide significant benefits in such areas as sensors and controls for automobiles and aircraft, high-power switching devices for the electric power industry, electric vehicles, and control electronics for the nuclear power industry. Silicon-based devices will not be sufficient for many applications operating at temperatures above 300°C such as power-conditioning devices in high temperature control systems. These devices will have to be produced from another material system. The intrinsic carrier concentration at any given temperature decreases exponentially with increasing band gap. The intrinsic carrier concentration of Si reaches $10^{15}cm^{-3}$ at about 300°C, GaAs reaches this intrinsic carrier concentration at about 500°C and GaN at about 1300°C. This makes GaN material attractive for high-temperature applications. High-power applications require high breakdown fields. The breakdown field of GaN is $3x10^6$ V/cm as compared to 2 and $4x10^5$ V/cm for Si and GaAs, respectively. For these reasons, the III-nitride devices can be used as high-temperature and high-power applications thus making it possible to reduce the weight and cost of the systems associated with cooling.

Early III-nitride research had a number of problems that prevented growth of high quality materials. These problems were lack of a good lattice matched substrate material, an inability to grow p-type GaN and lack of a suitable etching chemistry. Single-crystal GaN is not easily grown in bulk form. No commercial nitride substrates exist today for the epitaxial growth of AlGaInN-based devices. Most thin films and devices are therefore grown epitaxially on sapphire (Al_2O_3) or silicon carbide (SiC) substrates. The large differences in lattice constants and thermal expansion coefficients between the sapphire or SiC substrates and the AlGaInN-based semiconductors have made it difficult to grow high quality nitride films. In general, wide bandgap materials, such as GaN, are relatively difficult to dope, due to the presence of shallow donors and to the depth of the acceptor levels in the bandgap. Thus highly conductive p-type nitride alloys have been very difficult to produce due to the high n-type background concentration and minimal p-type dopant activation. In the last decade, great progress has been made in reducing the background electron concentration. Use of optimized buffer layer growth on sapphire substrates and the availability of better lattice and thermally matched SiC have allowed greatly improved layers to be grown.[3,4] Furthermore, improved epitaxial growth techniques have reduced the background electron concentration to as low as $\sim 10^{16}\text{cm}^{-3}$ in unintentionally doped GaN. P-type doping in Mg doped GaN has been achieved with carrier concentrations as high as $\sim 3\text{x}10^{18}\text{cm}^{-3}$ resulting from converting passivated Mg doped GaN into conductive p-type material by using low-energy electron beam irradiation (LEEBI) and thermal annealing under an N_2 ambient.[5,6]

Although there is no acceptable wet chemical etchant for GaN, various dry-etching techniques have proven reliable and convenient for etching nitride materials. There are still many areas which should be improved in III-nitride device technology such as increasing dopant incorporation and activation to improve p-GaN ohmic contacts, epitaxial lateral overgrowth (ELO) to reduce dislocation density, and improving the quality of the insulator (or oxide) layer which can be used as gate material in GaN metal insulator semiconductor field effect transistors (MISFETs) or metal oxide semiconductor field effect transistors (MOSFETs). Improvement in these all areas can be achieved by improving the quality of surfaces and interfaces by preparing clean and ordered nitride surfaces.

1.2 Importance of Surface States

III-nitride device technology like other advanced semiconductor device technologies will most likely require multiple processing and regrowth steps such as the etching/regrowth process in ELO, regrowth of ohmic contact layers, deposition of gate dielectrics, and several layers of photolithography and dry-etch patterning to define active device areas. The surface before epitaxial regrowth must be clean and smooth for the fabrication of electronic and photonic devices since interface states and impurities such as carbon (C) and oxygen (O) can degrade the quality of the regrown device.[7]

Table 1-1. Relative bond strengths of constituents commonly found in MBE, MOCVD and MOMBE growth.[8]

Bond	**Bond strength (kcal/mole)**
In-O	<77
Ga-O	85
Al-O	122
As-O	115
N-O	151
Me-In(Me)$_2$	49
Me-Ga(Me)$_2$	63
Me-Al(Me)$_2$	75
Me-As(Me)$_2$	67
Me-N(Me)$_2$	75

Nitride materials are particularly efficient for gettering C and O, as C and O are more strongly bonded to nitrides than to conventional III-V semiconductors. Thus it may require higher energy to remove these impurities from the III-nitride surfaces. Table 1-1 compares the bond strengths of some common constituents. As the bond strength of the atoms increases, the probability of their bonding or incorporation rate of impurity increases.

The surface of an air exposed or processed semiconductor has a large density of surface states which can result in a large surface recombination velocity and pinning of the Fermi level. At the semiconductor/semiconductor, semiconductor/metal or semiconductor/insulator interface, the lattice of the bulk semiconductor and all the properties associated with its periodicity terminate. As a result, localized states, called surface states, with energy in the forbidden energy gap of the semiconductor are introduced at or very near the interface. The localized surface states are illustrated schematically in Figure 1-1.

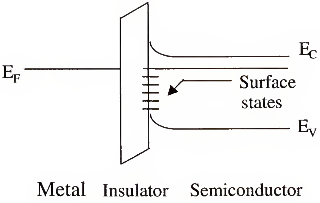

Figure 1-1. Schematic energy-band diagram of an MIS structure, illustrating the presence of surface states.

The interface states are distributed in energy; that is, they are described by a density of states, D_{it} [states/cm^2·eV]. At equilibrium, the occupancy of the interface states is determined by the semiconductor Fermi level. There are typically two kinds of surface states within the band gap of compound semiconductors (some that are donor-like and some that are acceptor-like). The acceptor-like states are in the upper half of the band gap and the donor-like states are in the lower half. Thus the interface is neutral when the Fermi level is near midgap. It has been reported that N vacancies can act as donors in GaN and that Ga vacancies act as acceptors.[9,10] The electrical characteristics of a device are very sensitive to the density and properties of these surface states at its interface. These surface states can reduce the conduction current in a device by trapping electrons or holes. Furthermore, the trapped electrons or holes can act like charged scattering centers, located at the interface, for the mobile carriers in a surface channel, and thus lower their mobility, ultimately reducing channel current. Surface states can also act like generation-recombination centers, or assist in the band-to-band tunneling process, and thus contribute to the leakage current in a gated-diode structure. As the density of interface-trapped charge changes with changes in the surface potential, it gives rise to an additional capacitance component in parallel with the bulk semiconductor capacitance. Surface states cause a detrimental effect on the optical and electronic properties of semiconductor devices. These surface states limit the performance of practical devices such as light emitting diodes (LEDs), solar cells and heterojunction bipolar transistors (HBTs) by providing nonradiative recombination centers or channels for surface or interface recombination. A highly reliable gate dielectric layer is one of the key issues for GaN MISFET technology. Its integrity is greatly influenced by surface pretreatment of the GaN layer as well as its growth conditions. A contamination-free surface and control of the native oxide are required to grow a high quality dielectric layer. Also, the incorporation of contaminants or an increase in surface roughness during processing steps before deposition of the gate oxide in metal oxide semiconductor field effect transistors (MOSFETs) will degrade device properties such as threshold voltage, breakdown voltage and peak mobility.[11-13] In any device-fabrication process, therefore, surface contamination and degradation must be avoided. Surface states can be minimized by various methods, including the use of surface chemical cleaning or the use of a passivation layer at the surface. Many conflicting results have been reported for surface states in GaN. Some reports claim that surface states in GaN do not pin the Fermi level and thus the ideal Schottky limit is applicable.[14] Dependence of the Schottky barrier height (SBH) on the metal work functions for n-GaN was studied by Bermudez et al.[15] and they found that the Schottky model was applicable to n-GaN where the SBH was given by the difference between the metal work function and the semiconductor electron affinity. On the other hand, Guo et al.[16] reported that the SBH for n-GaN was independent of the metal work function. This result suggests that the surface states or process-induced defects do pin the Fermi level. Also, Sun et al.[17] identified shifts in the surface Fermi level due to surface treatment. HCl-treated p-GaN surfaces showed a shift of the surface Fermi level toward the conduction band edge by ~0.9eV with respect to the thermally cleaned surface. Compared to the HCl-treated surface, the surface Fermi level on the KOH-treated surface lay ~1.0eV closer to the valence band edge, resulting in a much smaller surface barrier height to p-GaN than to the HCl-treated surface. Kim et al[18] could reduce 0.2-0.3eV of the SBH after removing 20Å of surface oxide using boiling aqua regia (HNO_3:HCl=1:3) for 10 min. This decrease of the SBH was calculated based on the following equation;[19]

$$q\phi_B = q\phi_{Bo} + 2kT(2m\chi)^{1/2}\cdot\delta/h/2\pi$$

where ϕ_B is the SBH, δ is the thickness of the insulating layer at the interface, ϕ_{Bo} is the SBH at the interface without a surface oxide, m is the mean tunneling effective masses of carriers, χ is the mean tunneling barrier for carrier injection from metal to semiconductor, h is Plank's constant and k is Boltzmann's constant.

1.3 Review of Surface Chemical Treatments

In semiconductor device technology, surface-cleaning procedures have been devised to (a) degrease and remove gross contamination, (b) remove particles and metal contamination and (c) remove surface oxide and carbon to provide an atomically clean surface. Usually the semiconductor surface is first degreased using conventional organic solvents (acetone and methanol). Metal contamination is then removed by using an H_2SO_4/HNO_3 solution. Next, a wet chemical treatment is performed to remove the surface oxide by using HF or HCl. However, a clean surface cannot be achieved with these wet chemical treatments alone due to possible contamination from the atmosphere and chemical residuals. In the case of ex-situ chemically cleaned layers, the re-oxidized layer generated after air exposure and chemical residuals has to be removed by suitable treatment before regrowth. Another surface cleaning method is to perform a wet chemical treatment outside the ultra high vacuum (UHV) chamber followed by a high-temperature thermal desorption step in-situ immediately before the regrowth process. The problem with this procedure is that it is not completely effective at removing carbon. Also, high temperature thermal desorption often induces undesired side effects such as dopant diffusion and roughening of the surface due to desorption of volatile surface atoms.

Recently, many research groups reported studies of in-situ chemical treatments of semiconductors using different gaseous sources. Improved electronic properties of GaAs surfaces were reported based on thermal treatment under a PH_3 over pressure.[20] Also, in-situ cleaning of GaAs, AlGaAs, InGaAs and InSb surfaces in UHV conditions using various hydrogen sources have been used to obtain high quality interfaces.[21-25] Hydrogen plasma treatments can remove the stable native oxide and carbon contaminant. Surface cleaning also can be achieved by using chlorine-based etching processes. Mui et al.[26] reported high-quality etched/regrown GaAs interfaces using in-situ Cl_2 etching. They reported in-situ cleaning of GaAs and InP using $AsBr_3$, $AsCl_3$ and PCl_3 before regrowth in the same chemical beam epitaxy (CBE) chamber, minimizing possible contamination in the etched/regrown interface.[27-34] Under these cleaning processes, it was possible to obtain surface morphology comparable to that of the as-grown surface. The in-situ chemical beam etching of (Al, In)GaAs, InP and GaSb using trisdimethylaminoarsenic (TDMAAs), trisdimethylaminophosphorus (TDMAP), and trisdimethylaminoantimony (TDMASb) provided a very smooth etched surface at the nanometer scale and a clean etched/regrown interface for regrowth applications.[35-43]

In III-nitrides, a number of studies have been reported for substrate cleaning and nitridation for buffer layer formation to reduce the effects of large mismatch in the lattice constants and thermal expansion between substrate and nitrides. The initial nitridation process of the substrate (Si, SiC, GaAs, Al_2O_3) before starting nitride growth is very critical for achieving better film quality.[44-49] However, there have been fewer studies in oxidation and cleaning of AlN and GaN surfaces. Ishikawa et al.[50] reported the results of XPS experiments to analyze the chemical composition of the contamination layer at the as-grown GaN surface. The results showed a contamination layer with a thickness ~ 2 nm consisting of gallium oxide and adsorbed carbon or hydrocarbon after air exposure. Both HCl-based and KOH-based treatments were effective in the removal of the surface oxide and other carbon-containing contaminants.[51] The oxidation of single crystal GaN in dry air has been investigated.[52] The thickness of oxide layers grown in dry air at 450°C and 750°C for up to 25 hours was only slightly thicker than that of the native oxide formed at room temperature on exposure to air. On increasing the temperature to 900°C, 5000Å thickness of the oxide layer was formed after 25 hours. Watkins et al.[53] found that GaN exhibits little oxidation until 10^5 Langmuir ($1L = 10^{-6}$ Torr) of oxygen exposure. The oxidation saturated on the surface to an atomic concentration of 10% at an exposure of 10^8 L, while oxidation in GaAs continued into the bulk above atomic concentration 20% after an oxygen exposure of 10^8 L. The adsorption of oxygen at the wurtzite (0001) and (000-1) GaN surfaces was investigated.[54] Bermudez et al.[55] studied the adsorption of O_2 on GaN (0001)-(1x1) surfaces, and its effects on electronic structure. The clean GaN surfaces were prepared by N_2^+ sputtering followed by in-situ annealing at 900°C or in-situ deposition of Ga metal followed by thermal desorption. Exposure of the clean GaN surface to O_2 reduced band bending by 0.15 eV, and surfaces prepared by ex-situ wet-chemical cleaning using 1:10 NH_4OH:H_2O showed the band banding to be 0.5 eV less than on clean surfaces. Prabhakran et al.[56] found that the native oxide present on the surface of GaN thin films, grown by MBE using solid Ga and N_2 plasma sources, was predominantly in the form of Ga_2O_3. Etching the GaN in warm (50 ~ 60°C) NH_4OH for 15 min. reduced these oxides significantly. Edwards et al.[57] could effectively remove 20-50 Å of organic and inorganic contamination and some of the oxide layer from GaN, AlN and AlGaN using MEOH, NH_4OH and NaOH. However, oxide and carbon free surfaces could not be achieved by these wet-chemical treatments alone. Smith et al.[58] and King et al.[59,60] reported cleaning of AlN and GaN surfaces using various wet-chemical treatments followed by in-situ thermal desorption to remove carbon and oxygen. However, complete thermal desorption of all contaminants was not achieved even at a temperature of 900°C. Atomic hydrogen is known to be effective at removing carbon and other surface impurities as well as oxides. Unfortunately, hydrogen passivates the electrical activity of Mg acceptors in GaN[61] and decreases the carrier concentration for undoped AlGaN by passivation of positively charged donors with negatively charged hydrogen.[62]

1.4 Technical Rationale/Objective of this Study

In order to apply surface chemical treatments to the device fabrication process, the following conditions are required: (a) the complete removal of carbon and oxygen contaminants, (b) a flat surface after treatment, (c) the elimination of surface damage and (d) the avoidance of dopant passivation. Conventional wet-chemical cleaning and thermal cleaning cannot remove contaminants effectively. Ex-situ chemical treatments such as wet-chemical cleaning have possible contamination problems for the atmosphere and require additional surface treatments to remove residual contaminants resulting from wet-chemical cleaning. Also, high temperature thermal desorption cleaning processes can induce undesired side effects such as dopant out-diffusion and roughening of the treated surface due to the production of volatile species. Therefore, in-situ chemical treatment of the surface before regrowth is necessary to improve the quality of the interface, and ultimately to improve device performance and reliability.

Plasma treatment is an excellent surface-cleaning method. Plasma treatment of III-V semiconductor materials is commonly employed as a method of etching these materials, and, to a lesser degree, as a method of surface cleaning. Surface cleaning using hydrogen plasma would be a promising technique. A hydrogen radical beam can effectively remove surface carbon and oxygen without seriously etching the surface, and these treatments can be handled in UHV growth chamber. Atomic hydrogen can remove carbon and oxygen by formation of volatile CH_x and H_2O compounds, respectively. Hydrogen plasma treatment is possible, at lower temperatures than is possible for conventional thermal cleaning. Hydrogen cleaning may require subsequent processing to remove residual passivation. Thermal treatment should be performed to reactivate passivated dopants after hydrogen plasma cleaning. Nitrogen has to be supplied during thermal treatments to suppress loss of nitrogen from the surface. TDMAP ($P[N(CH_3)_2]_3$) is an alternative source for in-situ surface chemical treatment. In other III-V materials, TDMAP has been shown to efficiently remove surface carbon and oxide. It is thought that the atomic hydrogen released from TDMAP on III-V surfaces removes carbon and oxygen by formation of volatile CH_4 and OH species. It is likely to serve the same role in the case of the nitrides. One can expect TDMAP to be less toxic than PH_3 because of the absence of P-H bonds. Also, since decomposition of this compound produces a Group V species (P), it is expected to produce a stoichiometric surface by supplying phosphorus overpressure. Another potential chemical treatment is in-situ oxide removal using PCl_3. PCl_3 is injected directly into the growth chamber and allowed to react on the wafer surface. The use of PCl_3 over Cl_2 or HCl as the dry cleaning gas has advantages. Very high purity PCl_3 (99.999%) can be obtained readily. PCl_3 is less corrosive than HCl and Cl_2 gases, and also can provide a Group V overpressure preventing preferential loss of nitrogen.

The major advantage of this study is that all processing steps, surface cleaning, regrowth and surface analysis can be performed in UHV without exposure to air. In order to determine optimal conditions for surface cleaning before regrowth, in-situ characterization using reflection high energy electron diffraction (RHEED), and ex-situ characterization using auger electron spectroscopy (AES), secondary ion mass spectroscopy (SIMS) and scanning electron microscopy (SEM)/atomic force microscopy (AFM) will be used to investigate surface structure, morphology and composition. Current-voltage (I-V) measurement will be performed to study the effect of surface states and surface treatments on electrical characteristics of MIS diodes. The objective of this study is to investigate the effects of surface chemical treatments on the structural, chemical, electrical and optical characteristics of the surface, to correlate this structure with the quality of the subsequently regrown III-nitride epitaxial layers and to find the optimum conditions for surface treatment of nitrides in order to improve performance and reliability of III-nitride based devices. In order to accomplish this objective, several areas are of major concern in this study. These include complete removal of carbon, oxygen and chemical residuals from the nitride surface even after exposure to photoresist and providing an ideal surface for regrowth (i.e. a contamination-free, stoichiometric and atomically smooth surface). The approach of this study is to remove the contaminated surface using various wet-chemical treatments ex-situ, and then to replace this cleaned surface with a controlled oxide using UV/O_3 for complete removal of carbon from the surface. Next, to remove the oxide and remaining impurities via in-situ treatments which will include thermal heating, exposure to plasma (N_2, H_2) and chemical beams using PCl_3 and TDMAP.

CHAPTER 2
EXPERIMENTAL PROCEDURES

The AlN and GaN samples were grown epitaxially by metalorganic molecular beam epitaxy (MOMBE) or metalorganic chemical vapor deposition (MOCVD) on Si (100) and sapphire (0001) substrates, respectively. Dimethylethylaminealane (DMEAA), triethylgallium (TEG) or elemental Ga for MOMBE samples and trimethylgalium (TMG) for MOCVD samples, and radio frequency (RF) nitrogen plasma for MOMBE and NH_3 for MOCVD were used as Al, Ga and N sources, respectively. The thicknesses of the films were 0.22 μm for AlN and 1-2 μm for GaN. For ex-situ cleaning, solvents (acetone and methanol), acids (HF and HCl), KOH-based solution and UV/O_3 treatments were used for both AlN and GaN at room temperature. The AlN and GaN samples were rinsed in DI water and blown dry with N_2 after all wet chemical treatments. In order to remove carbon contamination from AlN and GaN surfaces, UV/O_3 exposure was performed with a Jelight UVO Cleaner using an Hg lamp positioned 1 cm from the sample surfaces. The samples were then mounted on 2" Si wafer using indium with a molybdenum sample holder for loading into the UHV system. For further removal of surface C and O and removal of wet chemical residuals, thermal, N_2 or H_2 plasma, PCl_3 and TDMAP treatments were conducted in a UHV MOMBE growth chamber at various temperatures. The actual temperatures reported in this study for in-situ surface treatments and regrowth were measured by the temperature of the backside of the wafer using a thermocouple. All the in-situ cleaning was performed after photoresist (PR) deposition/strip and ex-situ cleaning (solvents, acid and UV/O_3 treatments) to determine the suitability of the surface cleaning technique for device processing. PR was deposited using 2:1 photoresist (AZ 1350J): thinner (AZ 1500) with 4000 rpm for 30 sec and baked at 85°C for 20 min. The PR was stripped using acetone. In-situ cleaning was performed using various conditions. In-situ cleaning using plasma was performed at three different conditions: (1) pure thermal cleaning without plasma at 900°C for 5 min, (2) thermal cleaning with N_2 plasma at 750°C or 900°C for 5 min and (3) thermal cleaning with a H_2/N_2 plasma at 750°C for 5 min. Chemical beam cleaning using PCl_3 and TDMAP was performed at temperatures of 500°C to 650°C with or without N_2 plasma exposure for 10 min flow rates of 5 and 15 sccm, respectively. Thermal cleaning with or without N_2 plasma at temperatures of 500°C and 650°C for 10 min were conducted to compare the efficiency of surface cleaning using PCl_3 or TDMAP or pure thermal cleaning. After finishing the in-situ treatments, ~2000 Å of GaN was grown on the treated AlN and GaN samples in the Varian Gen II MBE system to prevent re-oxidation before material characterization, and to examine the surface morphology of the regrown layer. This GaN layer was grown using elemental Ga at an effusion cell temperature of 955°C and substrate temperature of 750°C to minimize exposure to hydrocarbons. The Group V nitrogen atoms were generated by an SVT Associates radio frequency (RF) plasma source, which was operated at 400W forward RF power and at 5 sccm flow. AES and SIMS were used to monitor the presence of surface or interface impurities before and after treatments. The AES spectra were obtained using a beam energy of 5 keV. SIMS analysis was performed at Charles Evans and Associates using a Cs^+ beam. In-situ RHEED using a beam energy of 10 to 15 keV and a current of

1-1.5 A was used to investigate removal of the surface oxide and surface roughness after various ex- and in-situ treatments. The surface roughness of the treated samples was studied with SEM and Digital Instruments Nanoscope AFM operated in tapping mode.

Also, the utility of various treatments was assessed by analysis of the electrical characteristics of the MIS diodes. An AlN layer was grown on the treated GaN in the Varian Gen II MBE system to create the MIS diode structure. DMEAA and RF N_2 plasma were used as Al and N sources at temperatures of 375°C for 20 min. The Group III metalorganic source, DMEAA, was transported by an He carrier gas flow of 10sccm. The thickness was ~250 Å. A metal multilayer of Ti/Al/Pt/Au (250/500/500/1000 Å) provided Ohmic contact to the GaN. This Ohmic metal was annealed to 400°C for 30 sec to activate the contact. The metal contact on the AlN was 1000Å of Au. The size of the contacts was defined by using a shadow mask with dimensions ranging from 70 to 1000 μm. I-V measurement was performed at different applied voltage HP 4145B to test the MIS diode.

CHAPTER 3
SURFACE CLEANING OF AlN

AlN is an interesting material because of its negative electron affinity, making it a candidate material for the emitter of cold-cathode emission devices. There have been several studies of the oxidation of AlN,[63-66] but a successful cleaning method for AlN has not been reported, as Al forms very stable carbides and oxides. Recently, King et al.[59] have reported ex-situ wet-chemical cleaning using HF followed by in-situ cleaning using H_2 plasma and NH_3 at high temperatures. Figure 3-1 shows AES survey spectra of AlN after various ex-situ surface chemical treatments. As expected, the as-received sample shows significant surface C and O contamination due to exposure to air. Exposure to PR further increases the amount of carbon at the surface, while wet-chemical treatment based on HF was very effective in reducing surface O on AlN. Significant amounts of residual F were observed. Complete F termination of the AlN surface is desirable after HF treatment, because nitride surfaces covered with F will prevent re-oxidation of the surface in air before regrowth and this F can be desorbed at much lower temperatures than both C and O.[59] However, as shown in Figure 3-2, a 3-min HF treatment reduced the O concentration only ~50% and left the C concentration a little higher than the original nonprocessed level.

UV/O_3 treatment was found to be an effective cleaning method to reduce the surface C contamination. As shown in Figures 3-1 and 3-2 and in Table 3-1 UV/O_3 exposure for 25 min or 50 min after an HF acid treatment reduced the C level by ~50% on the AlN surface. The sample treated two times sequentially with UV/O_3 exposure for 25 min after an HF acid treatment shows the best result for removal of C (as shown in Table 3-1). However, higher oxygen coverage and significant amounts of F were detected as compared to no detection of F for the sample exposed to UV/O_3 for 50 min. Longer exposure to UV/O_3 with an acid pre-clean did not further appreciably decrease the surface C coverage. The reactive oxygen species from the UV/O_3 exposure can lead to formation of volatile compounds via surface reactions with the organic contaminants,[67] and thus remove C from the surface along with the surface chemical residual, such as F, remaining after acid treatment. In the case of carbon it is also possible for the impurity to be trapped in the nitride material oxidized by the ozone and then removed when the oxide is removed. These results indicate that the UV/O_3 treatment is one of the most useful cleaning methods for the removal of carbon contamination left from photolithography processing or excessive handling in device fabrication.

In order to study the surface stoichiometry after ex-situ chemical treatment, AES Al peak-to-N-peak ratios from the AlN surfaces were examined. Table 3-1 shows AES peak-to-peak height ratios for the UV/O_3 and various wet chemically treated AlN surfaces. The Al/N ratio was reduced compared to that of the as-received sample after HF treatment. Because the oxide is composed mostly of Al bonded to oxygen (Al-O), the removal of Al-O with HF can reduce the Al concentration on the AlN surface. The decrease in the Al-to-N ratio points out the evolution of the AlN surface composition originally dominated by Al oxide toward a more stoichiometric one. The UV/O_3 treatment restored the Al to N ratio to levels approaching those in the as-received material, thus there does not appear to be any enrichment of the surface in the Group III element beyond that normally observed in the material after exposure to air. Neither removal nor restoration of the oxide layer worsened the surface roughness. As shown in Figure 3-3 the RMS roughness measured by AFM did not increase beyond that obtained for the as-grown sample.

For further removal of surface C and O, in-situ thermal surface treatments with N_2 or H_2/N_2 plasma were required. Figure 3-4 shows the surface atomic concentration of C and O as measured by AES on AlN after various combinations of wet chemical and thermal surface treatment. All samples were exposed to photoresist (PR) and were given the HF/O_3 clean before thermal treatment. Virtually any thermal treatment was successful in obtaining a carbon-free AlN surface within the detection limits of AES. By contrast, an oxygen-free AlN surface could not be obtained under any of the conditions tested, though the reducing ambient produced by the H_2/N_2 plasma did appear to be somewhat more effective. The low efficiency of oxide removal from the AlN surface even with H_2 and N_2 plasmas is most likely due to the high strength of the Al-O bond. Further in-situ treatments using chemical beams such as PCl_3 and TDMAP were performed in an attempt to obtain a clean AlN surface. These treatments were efficient for removing C and F at temperatures as low as 500°C. However, only slight removal of oxygen was observed, and the results were no better than those obtained using a high-temperature thermal treatment under an N_2 and H_2 plasma. More stringent cleaning methods are needed to obtain a clean AlN surface. Surface cleaning of AlN is very difficult because of the high surface reactivity of aluminum and the high strength of the Al-O and Al-C bond. In order to maintain a clean AlN surface, growth of a sacrificial passivation layer (GaAs, InP or GaP) on top of the AlN layer may be required. This passivation layer should be completely desorbed along with surface oxide during the heat treatment before the regrowth.

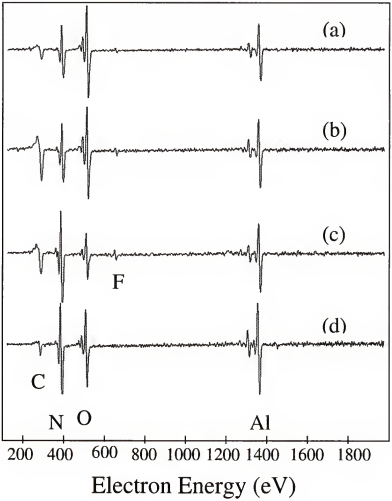

Figure 3-1. AES survey spectra of AlN (a) as-received, (b) PR deposit/strip, (c) acid cleaned for 3 min in 1:1 HF:DI, and (d) acid cleaned and 50-min UV/O_3 exposure.

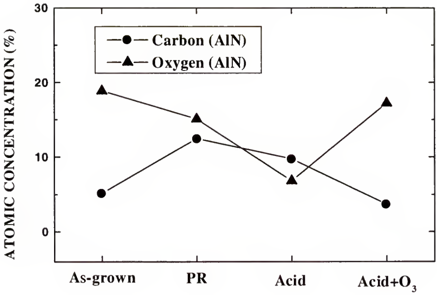

Figure 3-2. Surface atomic concentration of carbon and oxygen on AlN surface after various wet chemical treatments.

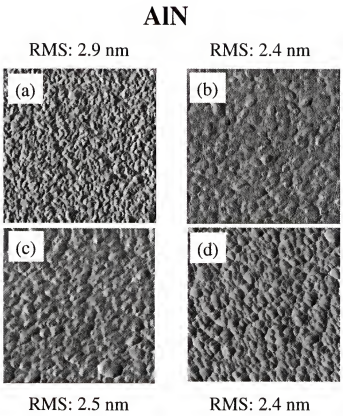

Figure 3-3. AFM images and RMS roughness values of AlN surfaces after various wet chemical treatments (a) as-received, (b) solvents (acetone/methanol, each 5 min), (c) 1:1 HF:DI, 3 min and (d) 1:1 HF:DI, 3 min and UV/O_3, 25 min.

Table 3-1. AES peak-to-peak height ratios for the UV/O_3 and various wet chemically treated AlN surfaces.

	C/N	**O/N**	**Al/N**	**F/N**
As-received	0.28	1.87	1.07	ND
PR/deposit/strip	0.76	1.66	1.16	ND
Solvents(acetone/methanol)	0.29	1.72	1.25	ND
1:1 HF:DI (3 min)	0.30	0.47	0.70	0.11
HF (3 min)/O_3 (25 min)	0.12	1.54	0.97	0.14
O_3 (25 min)/HF (3 min)	0.43	0.54	0.74	0.14
HF/O_3 (25 min)/HF	0.22	0.40	0.62	0.49
HF (3 min)/O_3 (50 min)	0.14	0.79	0.99	ND
HF/O_3 (25 min)/HF/O_3 (25 min)	0.09	1.07	0.93	0.16

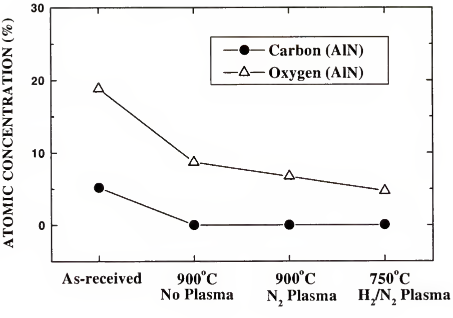

Figure 3-4. Surface atomic concentration of oxygen and carbon as measured by AES on AlN after various combinations of wet chemical and thermal surface treatment. All samples were exposed to photoresist (PR) which was followed by the HF/O_3 procedure before treatment.

CHAPTER 4
SURFACE CLEANING OF GaN

Oxygen atoms are actively adsorbed on the surface of III-V semiconductors, resulting in the production of a native oxide. A native oxide layer is also expected to grow upon air exposure after growth of GaN. Even though the native oxide does not grow as rapidly on the GaN surface as compared to other III-V semiconductors such as GaAs, the presence of oxides on the GaN surface can cause effects which are detrimental to device performance. The surface oxide layer acts as a barrier for carrier transport from metal to semiconductor, and subsequently increases the Ohmic contact resistivity. Also the oxide plays a role in increasing the Schottky barrier height at the surface. Furthermore, device fabrication processes involve several layers of photolithography and various etching processes to define active device areas. These processing steps result in carbon contamination and chemical residuals on the surface. The presence of the native oxide and contamination layer will also influence the integrity of the gate dielectric. The removal of the native oxide and generation of a contamination free surface is required to grow a high quality gate dielectric layer. In particular, carbon and oxygen are more strongly bonded to GaN than to other III-V semiconductors requiring more stringent cleaning techniques to obtain a clean GaN surface.

4.1 Ex-situ Cleaning

For ex-situ cleaning, solvents (acetone, methanol), acids (HCl, HF), KOH-based solution (AZ 400K developer) and UV/O_3 treatments were used. Figure 4-1 and Table 4-1 show AES survey spectra and peak to peak height ratios of GaN after various ex-situ surface chemical treatments. Similar to AlN, the as-received GaN sample shows significant amounts of carbon and oxygen on the surface. The PR deposit/strip procedure further increases the carbon contamination level on the surface, but produces the same level of oxygen. There is a small decrease in the oxygen level after solvent cleaning but little increase in the carbon level. A 1:1 HCl:DI solution was very effective for removing the native oxide. However, while this acid treatment was found to produce the lowest O/N ratio, significant amounts of carbon and chlorine were observed as shown in Table 4-1. UV/O_3 treatment was found be an excellent surface cleaning method to remove surface carbon contamination. As shown in Figure 4-1, an HCl acid treatment followed by UV/O_3 exposure for 25 min removed carbon and chemical residual (chlorine) completely from the GaN surface even for the case of photoresist exposed material. Preliminary evidence suggests that exposure to ozone does oxidize some of the GaN material. The combination of UV/O_3 oxidation and dipping in acid was also used to determine the best chemical cleaning method for removing carbon and oxygen from GaN surfaces. As shown in Table 4-1, UV/O_3 exposure for 25 min followed by an HCl acid treatment was very effective for oxide removal but left significant amounts of carbon. If UV/O_3 treatment is applied to the GaN surface with a native oxide, one can expect to effectively terminate dangling bonds and to replace Ga-C, Ga-H or Ga-OH bonds with G-O bonds. The oxide formed by treatment with an HCl solution followed by UV/O_3

treatment may be more uniform, reproducible, and stoichiometric than the native oxide. This may prevent re-adsorption of carbon or other impurities. However, UV/O_3 exposure followed by HCl treatment will remove this controlled oxide and allow adsorption of carbon atoms during air exposure.

AES Ga to N peak ratios from the GaN surfaces were investigated to study the surface stoichiometry changes after ex-situ chemical treatments as shown in Table 4-1. Similar to results in the AlN case, the Ga to N ratio was reduced ~40% compared to that of the as-received sample after acid HCl treatment. Since the oxide on as-received or UV/O_3 exposed sample surfaces is composed mostly of gallium oxide, the removal of this oxide layer with HCl can reduce the Ga/N ratio on the GaN surface. The UV/O_3 exposure again restored the Ga/N ratio to the levels of as-received material. As shown in Figure 4-2, the AFM results show that neither wet chemical treatments to remove oxide nor UV/O_3 exposure to restore the oxide layer increased the RMS roughness value beyond that of the as-received sample, though HCl treatment did appear to slightly planarize the GaN surface.

RHEED was used to study the removal of oxides and the surface roughness after various wet chemical treatments. Figure 4-3 shows RHEED patterns taken along the [11-20] azimuth on the GaN surfaces. No diffraction pattern was detected for the as-received and UV/O_3 exposed samples. This indicates that the native oxide and UV/O_3 generated oxide surfaces are likely to be amorphous. GaN surfaces treated in UV/O_3 oxidation followed by dipping in1:1 HF:DI or AZ 400K developer displayed (1x1) streaky RHEED patterns indicating removal of the UV/O_3 generated oxide or the native oxide and the generation of an atomically flat surface. However, these RHEED results do not indicate that HF and AZ 400K treated samples are completely free of oxygen or carbon contamination, as oxygen and carbon have been shown to be present on chemically cleaned GaN surfaces by AES and SIMS. RHEED results only indicate that the cleaned GaN surface is smooth and relatively free of oxides and other contaminants but significant amounts of oxygen and carbon contamination still exist. Also RHEED results indicate that native oxides do not grow rapidly on the GaN surface during the time (< 30 min) required to load the samples in the vacuum chamber. In summary, the lowest oxygen impurity levels on GaN surfaces were achieved after HCl based acid treatments, while UV/O_3 cleaning was very effective for removing carbon. However, complete removal of carbon and oxygen from the GaN surface could not be achieved by ex-situ chemical treatments only. No wet chemical treatment could remove oxygen completely from the GaN surfaces, and in-situ chemical treatments are required for further removal of carbon and oxygen from the GaN surface.

4.2 In-situ Cleaning

4.2.1. Thermal/Plasma Cleaning

For further removal of surface carbon and oxygen, in-situ surface treatments including thermal treatments with or without N_2 or H_2/N_2 plasmas were performed. All samples were exposed to photoresist and given the acid (HCl) and UV/O_3 clean before thermal treatment. After finishing the in-situ thermal treatments, GaN overgrowth using an elemental Ga and N_2 plasma was performed on the treated MOMBE grown GaN samples in a Varian Gen II MBE system to prevent re-oxidation before material characterization, and to examine the surface morphology of the regrown layer. The thickness of the overgrown GaN layer was ~100 nm for AES and ~200 nm for SIMS and SEM samples. Figure 4-4 shows the atomic concentration of carbon and oxygen as measured by AES on MOMBE grown GaN after various combinations of wet chemical and thermal surface treatment. Virtually any thermal treatment was successful in obtaining a clean GaN surface within the detection limits of AES. Figure 4-5 shows AFM images for the GaN capping layers regrown on MOMBE grown GaN samples exposed to various plasma treatments. None of the in-situ thermal cleaning processes significantly affected the roughness of the treated and regrown GaN surface.

Thermal cleaning techniques at lower temperature are desirable for many device structures such as heterostructure light emitting diodes and GaN/InGaN multi-quantum wells, where a low processing temperature is sought to preserve the integrity of the underlying InGaN devices layers and facilitate layer fabrication. For this purpose, the effect of thermal treatment with H_2/N_2 plasma on surface cleaning was investigated at lower temperature ranges from 500°C to 750°C. All samples were treated with PR/HCl/O_3 prior to H_2/N_2 plasma exposure. After H_2/N_2 plasma treatment MBE grown GaN was grown on treated MOCVD grown GaN at 725°C for 15 min. The thickness of the MBE grown GaN layer was ~75 nm. Figure 4-6 shows surface atomic concentration of carbon and oxygen as measured by AES on GaN after H_2/N_2 plasma exposure at different temperatures. As one can see, overgrowth on the sample which did not receive the H_2/N_2 plasma after exposure to the PR/HCl/O_3 treatment shows significant amounts of carbon and oxygen contamination at the interface. The surface carbon could be removed after H_2/N_2 plasma exposure only at 500°C. By contrast, the complete removal of oxygen was only achieved after H_2/N_2 plasma exposure at a much higher temperature of 750°C. SEM was used to examine the surface morphology of the H_2/N_2 plasma treated samples. Figure 4-7 shows SEM images of the GaN surfaces. Figure 4-7(a) is the surface image of the MOCVD grown GaN substrate. Figure 4-7(b), (c) and (d) show the regrown MBE GaN after H_2/N_2 plasma treatment at different temperatures. As can be seen in Figures 4-7(b) and (c), the regrown MBE GaN layers after H_2/N_2 plasma exposure at 500°C and 650°C show very smooth surfaces comparable to the MOCVD grown GaN substrate. However, the sample which was exposed to the H_2/N_2 plasma at 750°C shows a degraded surface as seen in Figure 4-7(d). This can be attributed to preferential loss of surface nitrogen by formation of volatile NH_X compounds or desorption of thermodynamically unstable GaN at high temperature and in high vacuum. This result indicates that the morphology of the MBE grown GaN is related directly to the surface structure of the MOCVD grown GaN substrate prior to regrowth. Slight degradation of the substrate after surface treatment can have significant impact on the properties of the subsequently grown layers. We did not observe this degradation for the MBE grown sample after H_2/N_2 plasma exposure at 750°C. Since the MBE grown GaN is very rough compared to the MOCVD sample, no surface morphology change could be seen even after very high temperature treatment. Contrary to AES data, as shown in Table 4-2, SIMS data reveals that a significant concentration of surface carbon and oxygen still exists after thermal or plasma treatments, and that more stringent cleaning methods are needed to obtain a clean GaN surface.

Figure 4-8 shows comparison of RHEED patterns between GaN surfaces for chemical treatments alone and for chemical treatments followed by thermal treatment in the MBE growth chamber taken along the [11-20] azimuth. After 700°C thermal treatment, the brightness and sharpness of the RHEED patterns were increased for both $HCl/O_3/HF$ and HCl/O_3/AZ 400K pretreated samples. This can be attributed to the further cleaning of the surface by desorption of adsorbed contaminants.

4.2.2. Chemical Beam (PCl_3, TDMAP) Cleaning

The experiments were performed in a Varian Gen-II molecular beam epitaxy (MBE) growth chamber. The substrates used in this study were undoped GaN grown on (0001) sapphire by metalorganic chemical vapor deposition (MOCVD) at Sandia National Laboratory. The film thickness and carrier concentration were 2.2 μm and $2x10^{17}cm^{-3}$. Trimethylgallium (TMG) and ammonia (NH_3) were used as Ga and nitrogen precursors. In order to demonstrate the effects of surface chemical treatments on the interfacial chemical characteristics and regrown GaN layer, photoresist (PR) deposit/strip, wet-chemical cleaning using solvents (acetone and methanol) and 1:1 $HCl:H_2O$ for 3 min, and UV/O_3 exposure for 25 min at room temperature were performed. After these ex-situ treatments, in-situ surface treatments was conducted using chemical beams in the ultra high vacuum growth (UHV) chamber for the further removal of surface impurities and generated UV/O_3 oxide. For in-situ chemical beam treatments, trisdimethylaminophosphorus (TDMAP) and phosphorus trichloride (PCl_3) were used at temperatures of 500 and 650°C with or without nitrogen plasma exposure for 10 min, and flow rates of 15 sccm for TDMAP and 5 sccm for PCl_3 using He as a carrier gas. The chamber pressure was 6 - $8x10^{-6}$ Torr during gas exposure. After finishing the in-situ treatments a 0.2 μm layer of GaN was grown on treated MOCVD GaN samples for 30 min at the same temperatures as those of the in-situ chemical treatments in order to prevent re-oxidation before material characterization, and to examine the surface morphology of the regrown layer. The rf nitrogen plasma was used as a nitrogen source and operated at a power of 400W and a nitrogen flux of 5 sccm. Elemental Ga was used as a Ga source in an effusion cell at a temperature of 955°C. The interfacial chemical compositions of the regrown samples were examined by AES using a beam energy of 5keV and SIMS using a Cs^+ beam (SIMS performed at Charles Evans and Associates). The surface morphology of the regrown layer was studied with a Digital Instruments Nanoscope Atomic Force Microscope (AFM) operated in tapping mode.

Figure 4-9 shows the SIMS depth profiles of impurities (carbon, oxygen and chemical residuals) for the MBE regrown GaN layers on MOCVD grown GaN substrates. In all samples considerable amounts of carbon and oxygen were detected in the near-substrate region even though most samples showed no evidence of carbon and oxygen by AES measurement. Only the sample grown at 650°C with N_2 plasma exposure during substrate heating to the growth temperature showed evidence of contamination by AES. The concentration of impurities near the interface is higher than in the regrown films. High levels of oxygen were present in all samples independent of the substrate treatments, possibly due to contamination from the N_2 plasma source. As shown in Figure 4-9(a), the sample grown at 500°C without any in-situ treatment before regrowth shows a high areal density of oxygen and carbon and ~0.1 μm of oxygen diffusion into the regrown layer from the substrate. This increase in the width of the interface may be due to the enhanced roughness of the surface of the regrown GaN at this low temperature (500°C) or to the absence of the N_2 plasma exposure during substrate heating to the growth temperature. This 3-dimensional columnar structure should also enhance diffusion of impurities. Figure 4-9(b) shows the SIMS depth profile for GaN grown at 650°C with N_2 plasma exposure during substrate heating to the growth temperature. This sample shows the highest peak level of carbon and oxygen contamination, but the peak is not located at the interface of the regrown layer. SIMS may just be plowing surface impurities ahead. Exposure to PCl_3 at 500°C for 10 min before regrowth reduced the interfacial C and O density as shown in Figure in 4-9(c). The sharper interface with a lower impurity level indicates that the PCl_3 treatment was more successful in removing the interfacial oxide. Unfortunately, significant amounts of phosphorus and chlorine were also found on the interface after PCl_3 treatment. After TDMAP treatment no significant reduction of impurities was observed and a high level of residual P was found.

In order to investigate the effects of chemical treatments on surface morphology of the regrown layers, AFM measurements were performed. Initially the surface morphology of the MOCVD grown GaN substrate was investigated. A tapping mode AFM image of the MOCVD grown GaN surface is shown in Figure 4-10. The surface displays deep trenches (~10 nm deep) and dislocation cores with an area root mean square (RMS) roughness value of 1.8 nm. Figure 4-11 shows an AFM image of the regrown MBE GaN layer at growth temperatures of 500°C and 650°C with or without N_2 plasma exposure during substrate heating to growth temperatures. As shown in Figure 4-11(a) the surface of the GaN which was regrown on MOCVD GaN at a growth temperature of 500°C is very rough, 15.4 nm RMS, and shows a 3-dimensional columnar structure. The reason for this high RMS value and columnar structure is most likely due to the low substrate temperature which results in a decrease in surface diffusion of atoms and the nucleation of small islands on top of the MOCVD grown GaN substrate. On the other hand, the regrown GaN at a growth temperature of 650°C shows lower RMS value regardless of N_2 plasma exposure during substrate heating as shown in Figure 4-11(b) and (c). This may be due to the increase in surface diffusion of atoms at the higher growth temperature. However, the regrown GaN layer without N_2 plasma exposure during substrate heating shows a rougher surface than the GaN regrown with N_2 plasma exposure. This may possibly be the result of high temperature heating without providing an overpressure of nitrogen to suppress preferential loss of the more volatile Group V element.

Figure 4-12 shows AFM images of the regrown GaN surface after in-situ surface chemical treatment using TDMAP. There was significant improvement in surface morphology and RMS roughness of the regrown layers after treatment. The regrown GaN at a growth temperature of 500°C after TDMAP cleaning without N_2 plasma exposure during substrate heating and cleaning showed the lowest RMS roughness value, 1.35 nm, and the best surface morphology as shown in Figure 4-12(a). This result indicates that the removal of surface impurities after TDMAP exposure increased the diffusion of surface atoms at the first stage of nucleation and increased the size of the islands. On the other hand, the regrown GaN surface after TDMAP cleaning with N_2 plasma exposure shows higher RMS roughness value than the one without N_2 plasma exposure. This may be explained by reduction of TDMAP arrival rate on the GaN surface due to blocking of TDMAP by N_2 plasma reducing efficiency of surface cleaning.

The effect of PCl_3 treatment on the regrown GaN surface morphology was also monitored by AFM as shown in Figure 4-13. For the sample treated with PCl_3 at 500°C without N_2 plasma the RMS rough value was 4.36 nm, and for the sample treated at 650°C with N_2 plasma the value was 9.6 nm. The removal of surface oxide after PCl_3 exposure is most likely related to the decrease of RMS roughness of the regrown GaN. However, PCl_3 treatment at 650°C with N_2 plasma made a rough surface and this affected the surface morphology of the regrown layer. This rough surface is possibly due to the removal of some GaN surface layer along with the oxide layer, but significant etching of the GaN using PCl_3 could not be obtained, even under conditions which could etch GaAs at a rate of 0.6 μm/hour.

4.3. Electrical Characteristics

The AlN/GaN metal insulator semiconductor FET (MISFET) is a promising candidate for high power and high frequency operation. The success of the AlN/GaN FET approach critically depends upon developing material with good structural properties and a low density of interface states. A contamination-free GaN surface and removal of the native oxide are required to grow a high quality dielectric layer.

The substrates used in this study were undoped GaN grown on (0001) sapphire by MOCVD. The film thickness and carrier concentration were ~2 μm and $\sim 10^{17} cm^{-3}$. The GaN surfaces were pre-treated with 1:1 $HCl:H_2O$ for 3 min and then UV/O_3 exposure for 25 min. For further removal of contamination, native oxide and UV/O_3 generated oxide, in-situ chemical treatments were performed at three different conditions: (1) thermal cleaning with N_2 plasma at 650°C for 10 min, (2) thermal cleaning with PCl_3 at 500°C for 5 min and (3) thermal cleaning with TDMAP at 500°C for 5 min. After finishing the in-situ treatments, ~250Å thickness of AlN layer was grown on the treated GaN in the Varian Gen II MBE system to create an MIS diode structure. DMEAA and RF N_2 plasma were used as Al and N sources at a temperature of 375°C for 20 min. Figure 4-14 shows the structure of the AlN/GaN MIS diode. After deposition of the AlN layer, part of the AlN was etched using a KOH based solution (AZ 400K developer) for 3 min to define the mesa structure. A metal multilayer of Ti/Al/Pt/Au (250/500/500/1000Å) was deposited on GaN to make an Ohmic contact. Au metal dots of 1000Å thickness were deposited on AlN using a shadow mask with dimensions ranging from 70 to 1000μm. The utility of various treatments was assessed by analysis of the electrical characteristics of the MIS diodes. I-V measurements were performed at different applied voltage using an HP 4145B to test this MIS diode. The surface morphology and roughness of the regrown AlN layers were investigated with AFM to find effects of various surface treatments on the surface structure of the regrown layer and to find effects of surface morphology on the electrical characteristics of the diode.

Figure 4-15 shows the I-V characteristics of the AlN/GaN MIS diodes after different surface pretreatments before AlN layer growth. Both as-received and PR/HCl/O_3 treated samples show similar current flow characteristics in forward and reverse applied voltages. The increase of the thickness of the insulator layer due to the surface native oxide or UV/O_3 generated oxide layer deareased the amount of current flow. The PR/HCl/O_3 treated diode shows smaller current flow than the as-received diode at high reverse applied voltages. This result indicates that the UV/O_3 generated oxide is more uniform and stable than the native oxide. After PCl_3 treatment at 500°C, the diode shows higher current flow in both forward and reverse directions. This can be attributed to the removal of the native oxide or UV/O_3 generated oxide.

Figure 4-16 shows I-V characteristics from the AlN/GaN MIS diodes after in-situ surface chemical treatment prior to growth of the AlN layers. As can be seen in Figure 4-16, the PCl_3 treated sample shows the best I-V characteristics. This result is possibly due to the higher quality of the AlN layer grown after PCl_3 treatment compared to AlN layers grown after N_2 plasma or TDMAP exposure. As can be seen in Figure 4-17 the AFM image of the AlN grown after PCl_3 exposure shows the best morphology and is comparable to the as-received MOCVD GaN substrate. This result indicates that the removal of surface impurities was achieved after PCl_3 exposure. This removal of surface impurities increased the diffusion of surface atoms during the AlN layer growth and made it possible to grow higher a quality AlN layer.

Based on SIMS and I-V results, ex-situ HCl/O_3 treatment followed by an in-situ PCl_3 chemical beam exposure was the most successful method for removing the interfacial carbon and oxygen. In order to find the optimum temperature for the PCl_3 treatment, GaN was exposed to PCl_3 at temperatures from 300°C to 600°C. In addition to the PCl_3 treatment, thermal cleaning without N_2 plasma exposure at 700°C was performed in order to compare the efficiency of the PCl_3 treatment with thermal annealing for the cleaning of the GaN surface.

The substrates used in this study were Si doped GaN grown on (0001) sapphire by MOCVD at Epitronics. The film thickness and electron concentration were 2 μm and $\sim 10^{18} cm^{-3}$. For the PCl_3 treated samples, the GaN surfaces were pre-treated with solvents (acetone, methanol) for 5min each, 1:1 HCl:H_2O for 3min, and UV/O_3 exposure for 25 min before loading the samples into the MOMBE growth chamber. For the thermal cleaning at 700°C sample, wet chemical exposure with 1:1 HF:H_2O for 3min was performed additionally after HCl/O_3 treatment to remove the oxide layer. After loading the samples, the GaN surfaces were exposed to PCl_3 at a flow rate of 5 sccm for 10min at temperatures from 300°C to 600°C, or to a 700°C thermal anneal for 10 min in vacuum. After finishing the in-situ treatments, a ~0.1 μm thick AlN layer was grown on the treated GaN at a growth temperature of 325°C for 1 hour. The AlN layer was used as a capping layer to prevent contamination of the treated GaN surface before SIMS measurement and also to form a gate dielectric for subsequent electrical analysis. Before the deposition of the gate dielectric material, pre-cleaning of the surface is required to reduce interfacial impurities or defects and to grow a high quality dielectric layer. I-V measurements were performed on the MIS diodes. After masking, part of the AlN was etched and Ti/Al (200/600 Å) was deposited on the GaN to make the Ohmic contact. Au metal dots were deposited on the AlN as the gate metal. The surface morphology and roughness of the regrown AlN layers and the PCl_3 treated GaN layers were investigated with AFM and the SIMS depth profiles of impurities were monitored to determine the degree of interface cleanliness after PCl_3 chemical treatment.

Figure 4-18 shows AFM images of the MOCVD grown GaN substrate and the AlN layers grown after PCl_3 exposure at different temperatures or thermal annealing at 700°C. As can be seen in Figure 4-18, all AlN surfaces show a 3-D granular structure while the MOCVD grown GaN substrate displays atomically flat and 2-D step flow growth. The increase of RMS value and 3-D granular structure is most likely due to the low substrate temperature during the AlN layer growth. The decrease in surface diffusion of atoms and the nucleation of small islands followed by 3-D columnar growth on the MOCVD grown GaN substrate increased the RMS value. Also, the AlN layer grown after PCl_3 exposure at 600°C shows the highest RMS value. This result is similar with that found in the case of the regrown GaN after PCl_3 exposure at 650°C. This result indicates that PCl_3 exposure above 600°C is too aggressive and degrades the surface morphology of the regrown layer.

Figure 4-19 shows the I-V characteristics of the AlN/GaN MIS diodes after PCl_3 treatment at different temperatures and thermal annealing at 700°C before the AlN layer growth. The diode treated with HCl/O_3 followed by PCl_3 exposure at 300°C shows the best I-V, and the diode treated with $HCl/O_3/HF$ followed by thermal annealing at 700°C shows the next best I-V characteristics (i. e. smaller leakage current and higher breakdown). This is most likely due to the decrease of the surface impurities or defects from the GaN surface and the better quality of the AlN layer growth after these surface cleaning methods. PCl_3 exposure above 400°C degraded the I-V characteristics of the diodes. The reason for the degradation of the I-V characteristics was assumed to be due to the generation of the surface damage after PCl_3 exposure above 400°C or to an increase in the concentration of interfacial impurities. However, PCl_3 exposure even at 500°C did not significantly affected the morphology and roughness of the treated GaN surface as shown in Figure 4-20. The above results of the I-V characteristics can be explained from the SIMS analysis data. As can be seen in Table 4-3, the sample treated with PCl_3 at 500°C shows a higher concentration of interfacial P and Cl but a lower concentration of O than that of the sample treated with PCl_3 at 300°C or treated with thermal annealing at 700°C. This increase in the concentration of interfacial impurities, P and Cl, is most likely responsible for the degradation of the diode.

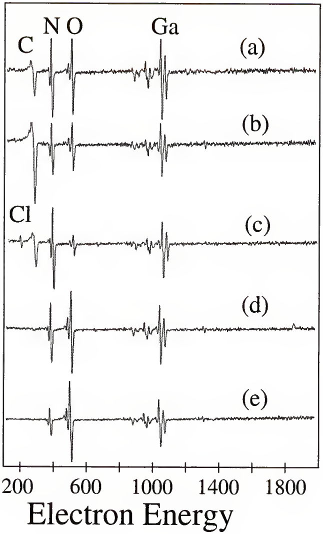

Figure 4-1. AES survey spectra of GaN (a) as-received, (b) PR deposit/strip, (c) acid cleaned for 3 min in 1:1 HCl:DI, (d) acid cleaned with 25-min UV/O_3 and (e) PR deposit/strip, acid cleaned and 25-min UV/O_3.

Table 4-1. AES peak-to-peak height ratios for the UV/O_3 and various wet chemically treated GaN surfaces.

	C/N	O/N	Ga/N	Cl/N
As-received	0.45	0.97	1.08	ND
PR/deposit/strip	1.66	0.95	1.05	ND
Solvents(acetone/methanol)	0.55	0.80	0.97	ND
1:1 HCl:DI (3 min)	0.40	0.24	0.64	0.14
HCl (3 min)/O_3 (25 min)	ND	1.47	1.00	ND
O_3 (25 min)/HCl (3 min)	0.13	0.26	0.68	0.09
HCl/O_3 (25 min)/HCl	0.06	0.45	0.79	ND

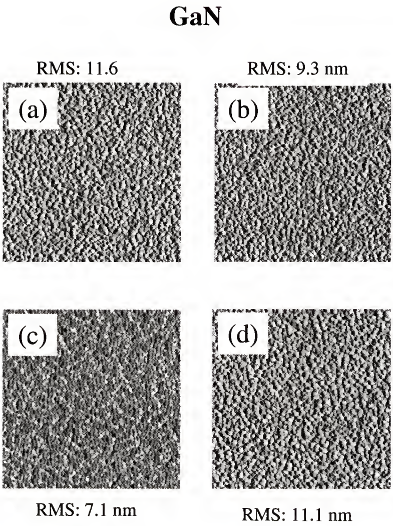

Figure 4-2. AFM images and RMS roughness values of GaN surfaces after various wet chemical treatments (a) as-received, (b) solvents (acetone/methanol, each 5 min), (c) 1:1 HCl:DI, 3 min and (d) 1:1 HCl:DI, 3 min and UV/O_3, 25 min.

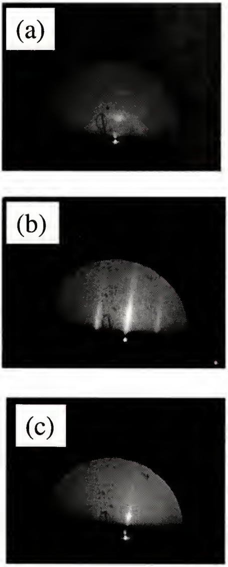

Figure 4-3. RHEED patterns taken along the [11-20] azimuth on the MOCVD-grown GaN surfaces after various chemical treatments (a) as-received GaN (b) HCl/O_3/HF-treated GaN and (c) HCl/O_3/AZ 400K-treated GaN.

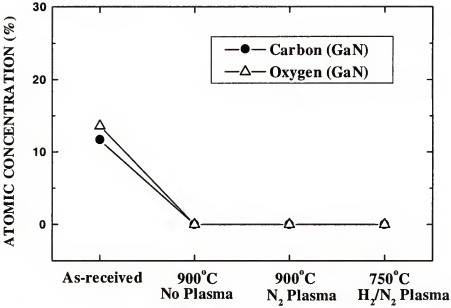

Figure 4-4. Surface atomic concentration of oxygen and carbon as measured by AES on GaN after various combinations of wet chemical and thermal surface treatment. All samples were exposed to PR which was followed by the HCl /O_3 cleaning procedure before treatment.

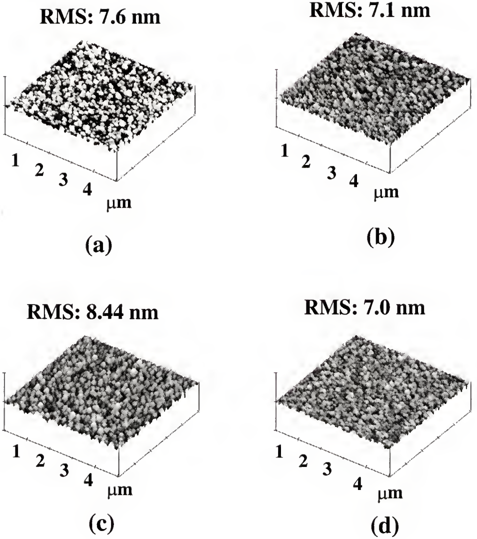

Figure 4-5. AFM images and RMS roughness values for regrown GaN capping layers on (a) as-received, (b) 5 sccm N_2 plasma exposure at 750°C for 5 min, (c) 5 sccm N_2 plasma exposure at 900°C for 5 min, (d) the mixture of 7.5 sccm H_2 and 2 sccm N_2 plasma exposure at 750°C for 5 min The (b), (c), and (d) samples were exposed to PR, 1:1 HCl:DI, 3min, and 25 min UV/O_3 before in-situ treatment.

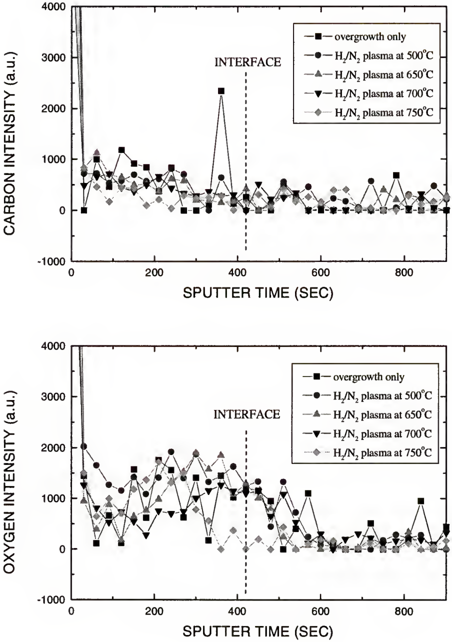

Figure 4-6. Surface atomic concentration of carbon and oxygen as measured by AES on GaN after H_2/N_2 plasma exposure at different temperatures. All samples were treated with PR/HCl/O_3 before plasma exposure.

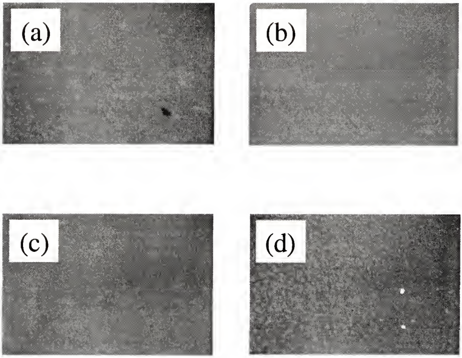

Figure 4-7. SEM images of GaN surfaces (15 kV, x10,000) (a) as-received MOCVD-grown GaN substrate and (b), (c) and (d) are MBE-regrown GaN on MOCVD-grown GaN substrate after exposure to H_2/N_2 plasma for 10 min at 500°C, 650°C and 750°C, respectively.

Table 4-2. Comparison of surface atomic concentration of C and O between AES and SIMS analysis on GaN after various combination of wet chemical and thermal surface treatment.

Method	AES		SIMS	
	C	O	C (cm^{-3})	O (cm^{-3})
As-received 750°C N_2 plasma	ND	ND	1.5×10^{21}	5.1×10^{21}
750°C N_2 plasma	ND	ND	3.2×10^{20}	2.0×10^{22}
750°C H_2/N_2 plasma	ND	ND	2.9×10^{20}	2.0×10^{22}

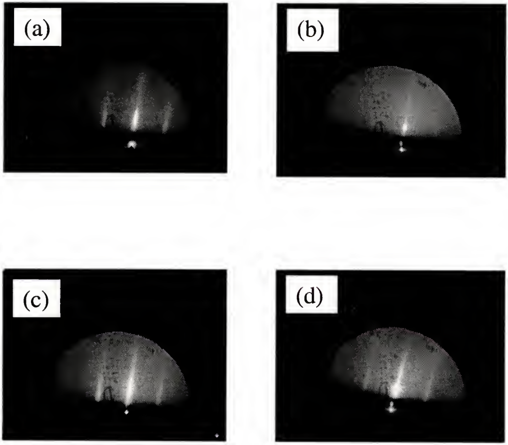

Figure 4-8. RHEED patterns taken along the [11-20] azimuth on the MOCVD-grown GaN surfaces after various chemical and thermal treatments (a) HCl/O_3/HF treated GaN, (b) HCl/O_3/AZ 400K-treated GaN, (c) HCl/O_3/HF treatment followed by thermal annealing at 700°C and (d) HCl/O_3/AZ 400K followed by thermal annealing at 700°C.

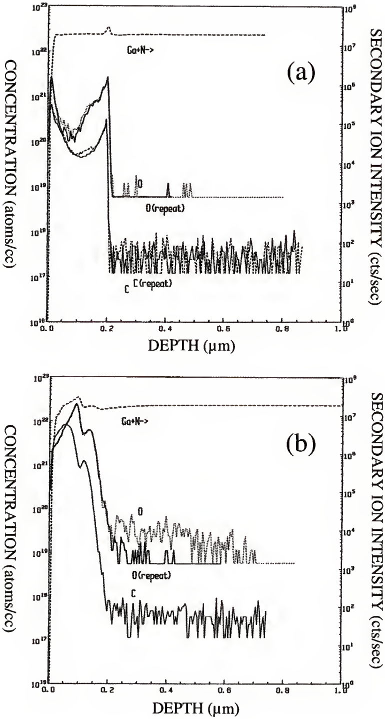

Figure 4-9. SIMS depth profiles of carbon and oxygen impurities for the MBE-regrown GaN layers on MOCVD-grown GaN substrates (a) overgrowth only at 500°C without N_2 plasma exposure and (b) overgrowth only at 650°C with N_2 plasma exposure during substrate heating to growth temperature.

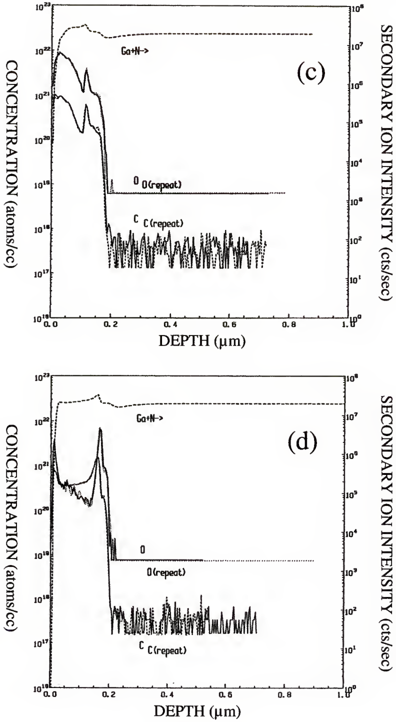

Figure 4-9. SIMS depth profiles of carbon and oxygen impurities for the MBE-regrown GaN layers on MOCVD-grown GaN substrates (c) PCl_3 exposure at 500°C for 10 min. and (d) TDMAP exposure at 500°C for 10 min. without N_2 plasma exposure before regrowth.

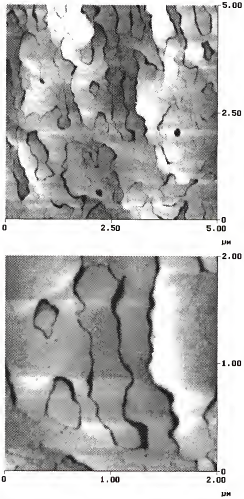

Figure 4-10. Tapping mode AFM images of the as-received MOCVD-grown GaN substrate. The RMS roughness value of this sample is 1.8 nm.

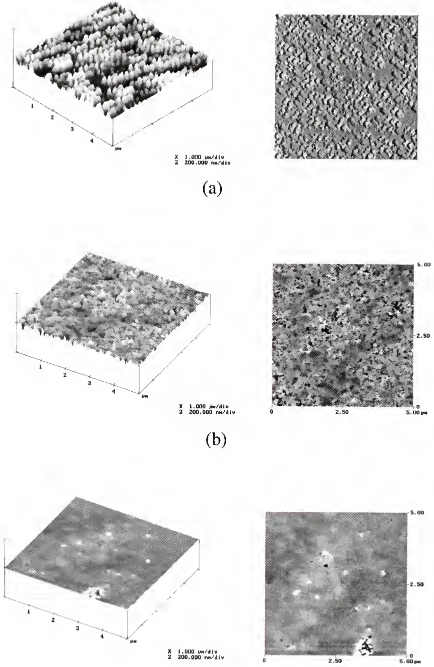

(a)

(b)

(c)

Figure 4-11. AFM images of the MBE-grown GaN layers on MOCVD-grown GaN substrates (a) overgrowth only at 500°C without N_2 plasma exposure, (b) overgrowth only at 650°C without N_2 plasma exposure and (c) overgrowth only with N_2 plasma exposure during substrate heating to growth temperatures. The RMS roughness values of (a), (b) and (c) are 15.5, 7.6 and 2.0 nm, respectively.

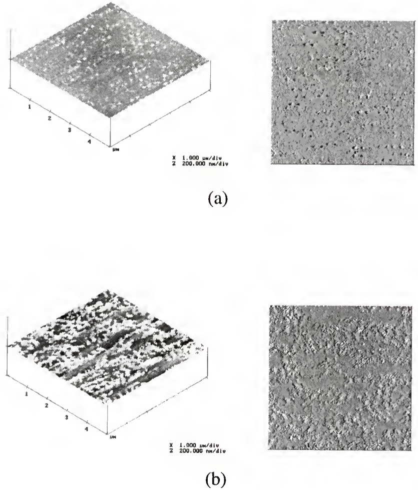

Figure 4-12. AFM images of regrown MBE GaN on MOCVD-grown GaN substrates after (a) TDMAP exposure at 500°C without N_2 plasma and (b) with N_2 plasma during substrate heating to growth temperature and TDMAP exposure. The RMS roughness values of (a) and (b) are 1.35 and 2.17 nm, respectively.

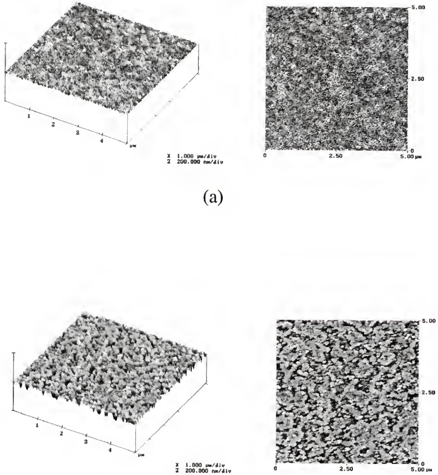

(a)

(b)

Figure 4-13. AFM images of regrown MBE GaN on MOCVD-grown GaN substrates after (a) PCl_3 exposure at 500°C for 10 min without N_2 plasma and (b) PCl_3 exposure at 650°C for 10 min with N_2 plasma exposure during substrate heating and PCl_3 exposure. The RMS roughness values of (a) and (b) are 4.36 and 9.6 nm.

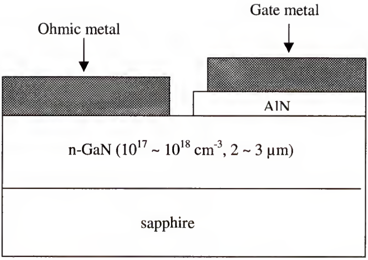

Figure 4-14. AlN/GaN MIS diode structure.

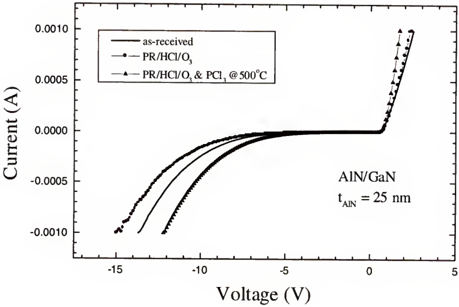

Figure 4-15. I-V characteristics from the AlN/GaN MIS diodes after surface pretreatment before growth of AlN layers.

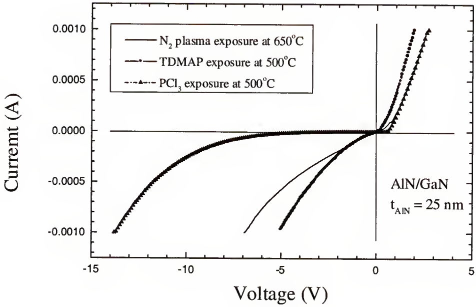

Figure 4-16. I-V characteristics from the AlN/GaN MIS diodes after in-situ surface chemical treatments before the AlN layer growth. The HCl/O_3 cleaning procedure was applied for all samples before in-situ treatment.

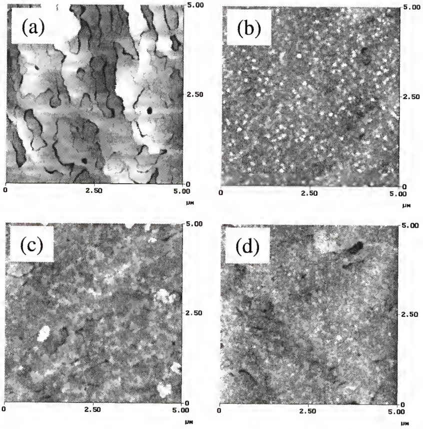

Figure 4-17. AFM images of (a) as-received MOCVD GaN, (b) AlN grown on MOCVD GaN after N_2 plasma exposure at 650°C for 10 min, (c) after PCl_3 exposure at 500°C for 5 min and (d) after TDMAP exposure at 500°C for 5 min of GaN before AlN growth. 1:1 HCl:H_2O and UV/O_3 cleaning were performed before thermal treatments for (b), (c) and (d) samples. The RMS roughness values of (a), (b), (c) and (d) are 1.83, 1.52, 1.55 and 1.09 nm, respectively.

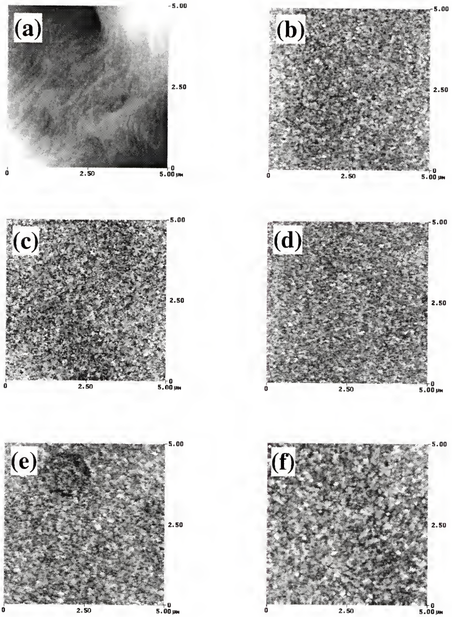

Figure 4-18. AFM images of (a) as-received MOCVD GaN, (b) AlN grown on MOCVD GaN after $HCl/O_3/HF$ followed by thermal annealing at 700°C, (c) after PCl_3 exposure at 300°C, (d) after PCl_3 exposure at 400°C, (e) after PCl_3 exposure at 500°C and (f) after PCl_3 exposure at 600°C. For (c), (d), (e) and (f) samples, HCl/O_3 treatment was performed before PCl_3 exposure. The RMS roughness values of (a), (b), (c), (d), (e), (f) are 0.87, 2.60, 2.81, 2.62, 2.57, 4.45 nm, respectively.

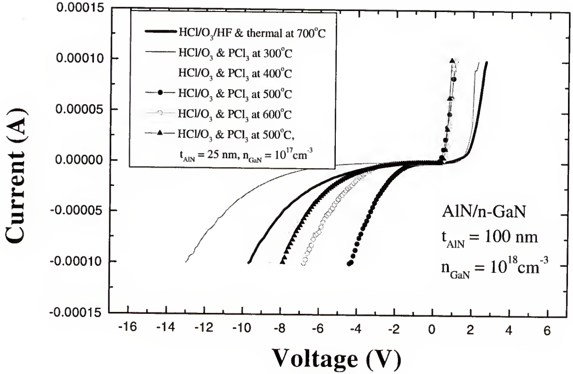

Figure 4-19. I-V characteristics from the AlN/GaN MIS diodes fabricated from samples from treated with various chemical procedures before AlN deposition.

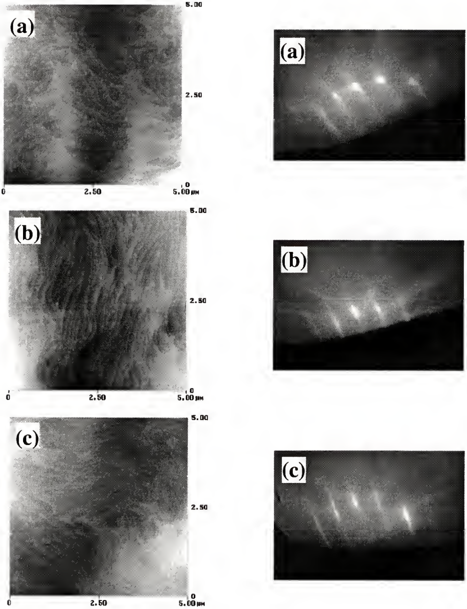

Figure 4-20. AFM (left) and RHEED (right) images of the MOCVD GaN (a) as-received, (b) after PCl_3 exposure at 300°C and (c) after PCl_3 exposure at 500°C. The RMS roughness values of (a), (b) and (c) are 0.72, 0.76 and 0.94 nm, respectively. RHEED patterns were taken along the [11-20] azimuth.

Table 4-3. Atomic concentration of interfacial impurities as measured by SIMS after various chemical treatments on the GaN before AlN deposition.

Method	C (cm^{-3})	O (cm^{-3})	Cl (cm^{-3})	P (cm^{-3})
HCl/O_3 500°C PCl_3	7 x 10^{20}	2.9 x 10^{20}	1.6 X 10^{20}	9.5 x 10^{20}
HCl/O_3 300°C PCl_3	2.9 x 10 ^{20}	6.5 X 10^{20}	1.6 x 10^{19}	2.6 x 10^{20}
$HCl/O_3/HF$ 700°C Anneal	2 x 10^{20}	5.5 x 10^{20}	2.6 x 10^{18}	2.5 x 10^{19}

CHAPTER 5
GENERATION AND REMOVAL OF THERMAL DAMAGE

GaN is a promising candidate material for high temperature/high power electronic devices because of its wide band gap, high breakdown field, high electron saturation velocity, and good thermal stability.[1,2] High temperature processing is required in a number of GaN device processing steps, including activation of implanted dopants,[68,69] removal of implantation induced damage,[70,71] alloying of Ohmic contacts, and oxide desorption from the GaN surface prior to regrowth. Further, in the GaN-based metal semiconductor field effect transistor (MESFET) technology, thermal stability of the Schottky diode[72-75] is one of the key issues. However, most work reported to date has focused only on the thermal stability of the Ohmic metal contacts.[76-78] It is also necessary to study the thermal stability of the epi-layer and methods for removal of the thermally damaged material. In an ion implanted GaN MESFET, for example, a Schottky gate metal contact must be formed on the implanted channel regions after the high thermal activation annealing. Any residual damage will produce leakage under the gate and severely compromise device performance. This work reports on a study of current voltage (I-V) and reverse breakdown voltage characteristics in GaN Schottky diodes as a function of annealing and post-anneal surface treatment.

Figure 5-1 shows the layer structures of the planar Schottky diodes used in this study. All of the layers were grown by rf plasma-assisted molecular beam epitaxy (MBE) at SVT Associates. For the n-GaN diode structure, 0.8μm of n^+-GaN (n ~$8x10^{18}cm^{-3}$) was grown on c-plane Al_2O_3 substrate, followed by growth of 3.2μm of undoped GaN (n ~$10^{16}cm^{-3}$). For the p-GaN diode structure, 2μm of undoped GaN (n ~$10^{16}cm^{-3}$) was grown on an Al_2O_3 substrate, followed by growth of 1μm of p-GaN (p ~$10^{18}cm^{-3}$). Ohmic metal contacts were formed with Ti/Pt/Au (400Å/200Å/1000Å) for n-GaN and Ni/Au (400Å/1000Å) for p-GaN. The Ohmic metal contacts were deposited using an electron beam evaporator and defined by lift off processing. After the Ohmic contact formation, the samples were annealed in a temperature range from 400°C to 900°C for 30 sec. under a nitrogen (N_2) ambient using rapid thermal annealing (RTA) in an AG Heatpulse 410 system. After annealing, each sample was divided into pieces and chemically treated. The procedure for chemical treatments was: UV/O_3 exposure for 25 min. followed by dipping into HCl:DI (1:1) solution for 3 min.. This process was performed 10 times repeatedly in an attempt to remove the damaged layer caused by thermal annealing. Next, Schottky metal was deposited with Pt/Au (300Å/1500Å) for n-GaN and Ti/Pt/Au (400Å/200Å/1000Å) for p-GaN through a shadow mask. The diameter of the contacts was 500μm. Prior to loading in an evaporator chamber the samples were cleaned in a solution of HCl:DI (3:1) for 1 min. to remove the native oxide from the GaN surface in order to ensure uniform contact properties upon subsequent deposition. Finally, the I-V characteristics were measured at room temperature using a HP4145B semiconductor parameter analyzer. Atomic force microscopy (AFM) and scanning electron microscopy (SEM) were used to observe the surface morphology before and after annealing and after chemical treatment. Auger electron spectroscopy (AES) was used to provide information regarding the composition of the surface.

Figure 5-2 shows the I-V characteristics from n-GaN Schottky diodes formed after annealing at different temperatures. The reverse breakdown voltages, V_{BD}, increase as the annealing temperature increases to 700°C. Upon annealing at 800°C, the V_{BD} decreases and after 900°C annealing the breakdown voltage decreases even further. Table 5-1 shows the summary of I-V characteristics of n-GaN Schottky diodes after annealing at various temperatures and chemical treatments. The I-V characteristics of the Schottky diode, $\O_B$ and n, were determined assuming thermionic emission:

$$I = I_s\,[e^{qV/nkT}-1] \quad \text{and} \quad I_s = AA^*T^2e^{-q\O_B/kT},$$

where I_s is the saturation current, A is the contact area, and A* is the effective Richardson constant ($24\text{A/cm}^2\text{k}^2$ for n-GaN and $72\text{A/cm}^2\text{k}^2$ for p-GaN based on $A^* = 4\pi m^*qk^2/h^3$ with $m^* = 0.20m_o$ for n-GaN and $m^* = 0.60m_o$ for p-GaN). T is temperature, q is the electron charge, k is the Boltzman constant, and V is the applied voltage. The breakdown voltage was arbitrarily taken to be the voltage at which the reverse current exceeded 5mA.

As the annealing temperature was increased to 700°C, $\O_B$ increased from 0.6eV to 0.65eV, while the ideality factor, n, decreased from 1.88 to 1.48. This increase in $\O_B$ and decrease in n after annealing at 700°C can be attributed to a reduction in the density of surface defects. After 900°C annealing, $\O_B$ is further reduced to 0.56eV. This Schottky barrier height reduction also causes a reduction in the reverse breakdown voltage. This may be due to preferential loss of nitrogen from the GaN surface after the high temperature annealing. Nitrogen vacancies are thought to increase the carrier concentration in GaN. This high surface carrier concentration might increase tunneling at the metal/n-GaN interface under reverse bias for the Schottky diodes and explain the increase in the reverse leakage. Also, the removal of the surface oxide and creation of surface damage after 900°C annealing can decrease $Ø_B$, ultimately decreasing V_{BD}. The SEM in Figure 5-3(b) shows a rough surface after 900°C annealing, again probably due to loss of GaN from the surface.

Figure 5-4 shows I-V characteristics from n-GaN Schottky diodes after annealing and ozone/HCl chemical treatments. AES depth profiles of the annealed sample suggest that nitrogen loss is occurring in the very near surface region. It was hoped that repeated ozone/HCl chemical treatment could remove this damaged layer whose thickness was believed to be ~100Å. However, this treatment significantly reduced the V_{BD} for samples annealed in the temperature range of 500 ~ 800°C as seen in Table 5-1. For those annealed at 600 ~ 800°C and chemically treated, the V_{BD} was reduced by ~60%. As shown in Figure 5-3 (c) and Figure 5-5, there are deep pits after annealing and the ozone/HCl treatment. This surface structure is most likely responsible for the apparent reduction of the barrier height and the reduction in V_{BD}, as it probably produces spiking of the metal. For samples annealed at 900°C and ozone/HCl treated there is some small recovery of V_{BD} due to the removal of the thermally damaged surface area. Also, the atomic concentration of oxygen on the surface of the sample treated by ozone/HCl is much lower than that on the air exposed sample. This removal of surface oxide might also reduce $Ø_B$ and V_{BD}.

For p-GaN Schottky diodes, the I-V curves exhibit very leaky behavior. The mechanism of current flow through the interface cannot be established and the exact value of the Schottky barrier height and ideality factor cannot be estimated. Figure 5-6 shows the reverse I-V characteristics for Ti/Pt/Au Schottky contacts on p-GaN samples after annealing at different temperatures. The reverse currents gradually decrease as the annealing temperature is increased to 700°C due to the removal of defects from the material and subsequent improvement of the quality of the Ohmic metal. Upon annealing at 800°C, the current begins to increase and further increases after 900°C annealing. This most likely can be attributed to the degradation of both the GaN and the Ohmic contact after high temperature annealing. The level of current flow in p-GaN Schottky diodes is very low even at high applied voltage as shown in Figure 5-7. This may be due to the high sheet resistance of the p-GaN material and the high contact resistance between the Ohmic metal and the p-GaN. At low current, as shown in Figure 5-8, the control sample does not show rectifying behavior. This leakage may be due to segregation of Mg on surface during epi-growth or to severe disorder on the p-GaN surface. Upon annealing at 900°C, the I-V curve again does not show rectifying behavior, but after ozone/HCl chemical treatment some rectification is observed.

For further removal of the damage caused by thermal annealing at 900°C, RF N_2 plasma exposure at 750°C or PCl_3 chemical beam exposure at 550°C for 10 min. was performed on the thermally damaged n-GaN surface. Figure 5-9 shows the I-V characteristics from n-GaN Schottky diodes after thermal treatment with N_2 plasma or PCl_3. The level of current flow for the Schottky diode exposed to N_2 plasma at 750°C is very high for applied small bias, giving Ohmic behavior. This result can be attributed to the very high surface carrier concentration due to the preferential loss of nitrogen, enhancing carrier tunneling at the metal/n-GaN interface. This preferential loss of nitrogen from the n-GaN surface might be caused by (a) thermal evaporation of more volatile nitrogen atoms from the surface at high vacuum and high temperature condition or (b) creation of n-type damage such as nitrogen vacancies by nitrogen ion sputtering after exposure to the high ion energy plasma (400W rf power) at 750°C. The diode exposed to PCl_3 also shows high reverse current flow at applied small reverse voltages and soft reverse breakdown behavior. This increase of reverse leakage current is most likely due to the preferential loss of surface nitrogen atoms by formation of volatile NCl_3 compounds or further increase of surface damage after exposure of thermally damaged n-GaN to PCl_3. Also, N_2 plasma or PCl_3 exposure after UV/O_3 oxidation and HCl oxide removal steps was investigated to study the removal of thermally damaged n-GaN. As shown in Figure 5-10, the sample treated with UV/O_3 and HCl procedures followed by PCl_3 exposure after 900°C annealing shows improvement of the Schottky diode characteristics due to the removal of damage. The reverse breakdown voltage of the diode was increased ~50% compared to that of the thermally damaged diode after 900°C annealing. The sample exposed to N_2 plasma after UV/O_3 and HCl treatment again shows a very high level of leakage current due to the conversion of the n-type GaN surface to very highly n-type GaN surface resulting tunneling of carrier in both directions at metal/n-GaN interface. In order to find the effect of surface roughness on the I-V characteristics of the diodes, surface morphology was examined by SEM. Figure 5-11 shows the SEM images of the n-GaN surface after N_2 plasma or PCl_3 exposure with or without UV/O_3 and HCl procedures for thermally damaged n-GaN. After PCl_3 exposure no significant surface morphology change was found. The creation of n-type defects or removal of damage from the surface was probably achieved at the microscopic level, thus one could not obtain any result that can explain relation between the structural and electrical properties with very rough n-GaN surface. On the other hand, the samples exposed to the N_2 plasma displays more flat surface structures with deep pits. This can be attributed to the reconstruction of the surface with N_2 plasma exposure at 750°C. Based on I-V characteristics for the N_2 plasma exposed samples, even the relatively flat surfaces may include significant amounts of n-type defects such as nitrogen vacancies.

In summary, annealing in N_2 ambients and surface chemical treatments were shown to affect the electrical properties of GaN Schottky diodes. Annealing at a temperature of 700°C produced the best I-V characteristics in both n- and p-GaN Schottky diodes. Upon annealing at 900°C, the reverse diode characteristics were significantly degraded. The preferential loss of nitrogen from the GaN surface after high temperature annealing most likely increased the surface carrier concentration. This high surface carrier concentration then increased the reverse leakage current of the Schottky diodes, enhancing tunneling at the metal/GaN interface under reverse bias. The ozone/HCl treatment after 500 ~ 800°C annealing induced significant reduction of the breakdown voltage, most likely due to the degradation of the surface structure. For samples annealed at 900°C and ozone/HCl treated there was some small recovery of breakdown voltage due to the removal of the thermally damaged surface area. The sample exposed to N_2 plasma at 750°C after being thermally damaged shows the worst Schottky diode characteristics due to the highly increased surface carrier concentration. PCl_3 exposure removed the thermally damaged surface and increased the reverse breakdown voltage.

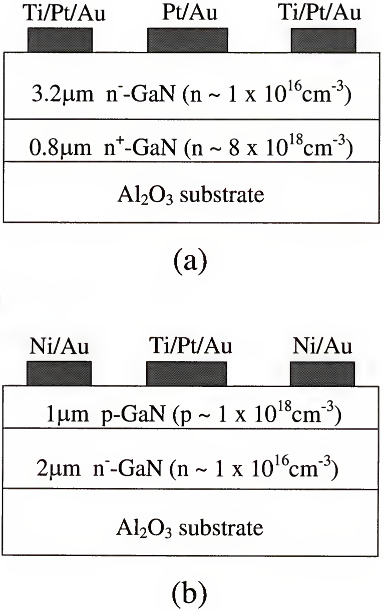
Ti/Pt/Au
Pt/Au
Ti/Pt/Au
3.2μm n^--GaN ($n \sim 1 \times 10^{16} cm^{-3}$)
0.8μm n^+-GaN ($n \sim 8 \times 10^{18} cm^{-3}$)
Al_2O_3 substrate
(a)
Ni/Au
Ti/Pt/Au
Ni/Au
1μm p-GaN ($p \sim 1 \times 10^{18} cm^{-3}$)
2μm n^--GaN ($n \sim 1 \times 10^{16} cm^{-3}$)
Al_2O_3 substrate
(b)

Figure 5-1. Layer sructures of the planar Schottky diodes (a) n-GaN Schottky diode and (b) p-GaN Schottky diode.

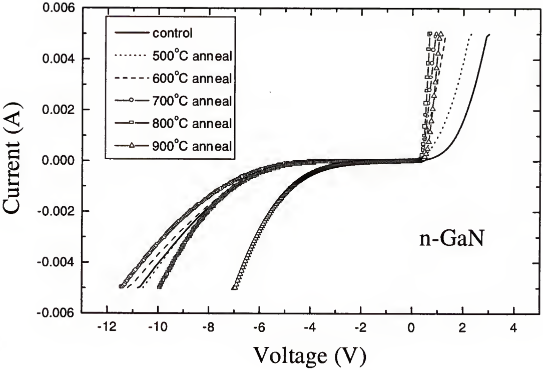

Figure 5-2. I-V characteristics from the n-GaN Schottky diodes formed after annealing at different temperatures.

Table 5-1. Summary of characteristics of n-GaN Schottky diodes.

Diodes	SBH (eV)	n	V_{BD} (V)
control	0.60	1.88	-10.8
500°C	0.62	1.69	-10.6
600°C	0.62	1.54	-11.2
700°C	0.65	1.48	-11.5
800°C	0.59	1.99	-9.9
900°C	0.56	2.10	-7.0
500°C/T	0.64	1.67	-8.8
600°C/T	0.60	1.56	-3.4
700°C/T	0.51	2.54	-3.5
800°C/T	0.61	1.76	-3.9
900°C/T	0.56	2.00	-8.2

* T indicates ozone/HCl treatments.

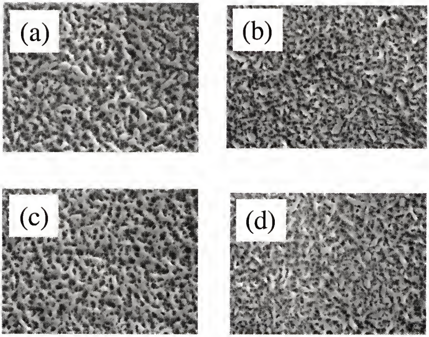

Figure 5-3. SEM images of the n-GaN surface (a) after annealing at 400°C, (b) after annealing at 900°C, (c) after annealing at 400°C followed by ozone/HCl treatment and (d) after annealing at 900°C followed by ozone/HCl treatment.

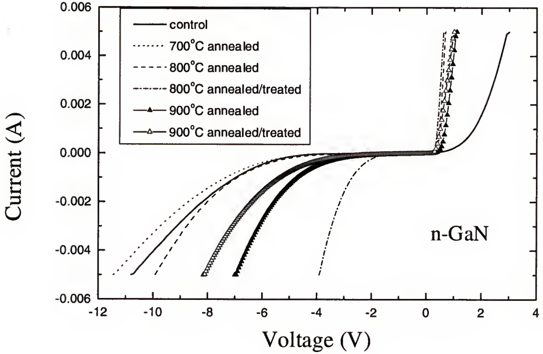

Figure 5-4. I-V characteristics from the n-GaN Schottky diodes after annealing and ozone/HCl treatment.

as-received

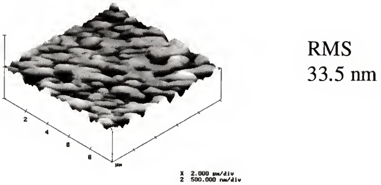

800°C annealed

800°C annealed/treated

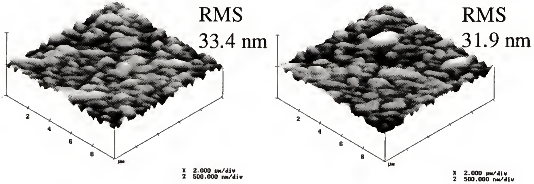

900°C annealed

900°C annealed/treated

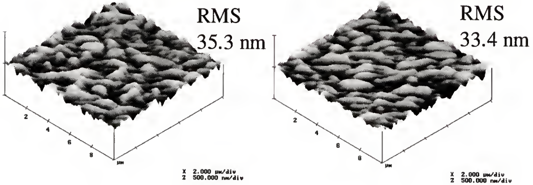

Figure 5-5. AFM images of n-GaN surface after annealing and ozone/HCl treatment.

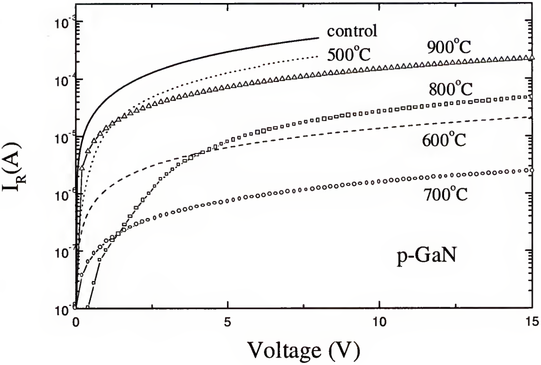

Figure 5-6. Annealing temperature dependence of the reverse I-V characteristics of the p-GaN Schottky diodes.

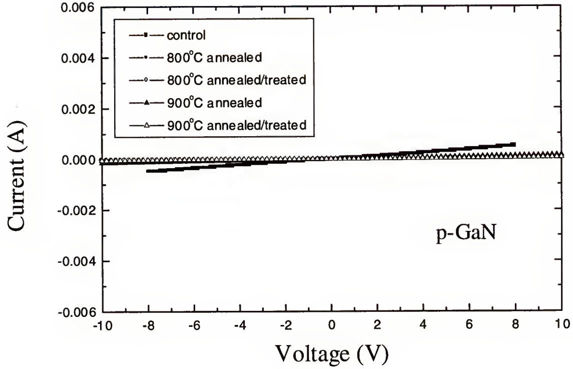

Figure 5-7. High current I-V characteristics from the p-GaN Schottky diodes after annealing and ozone/HCl treatment.

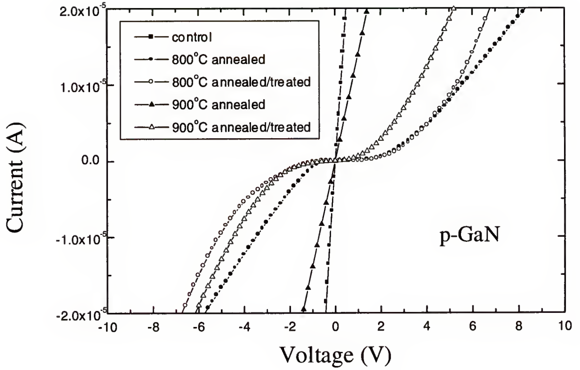

Figure 5-8. Low current I-V characteristics from the p-GaN Schottky diodes after annealing and ozone/HCl treatment.

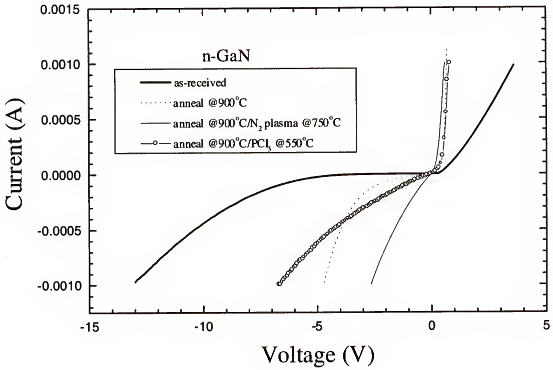

Figure 5-9. I-V characteristics from n-GaN Schottky diodes annealed at 900°C or annealed at 900°C and then O_3/HCl procedures followed by N_2 plasma or PCl_3 exposure.

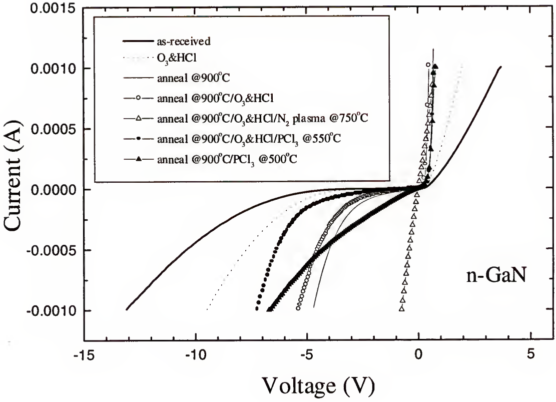

Figure 5-10. I-V characteristics from n-GaN Schottky diodes annealed at 900°C or annealed at 900°C and then O_3/HCl procedures followed by N_2 plasma or PCl_3 exposure to remove thermally damaged layers.

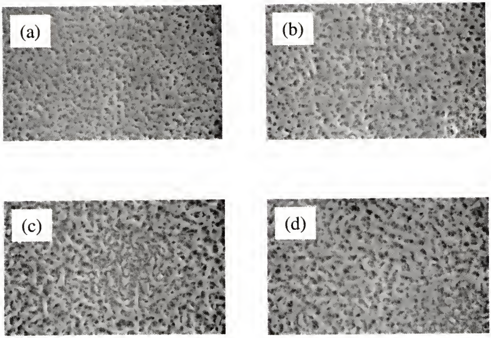

Figure 5-11. SEM images of n-GaN surface for annealed at 900°C followed by (a) N_2 plasma exposure at 750°C for 10 min, (b) O_3/HCl procedures and then N_2 plasma exposure at 750°C for 10 min, (c) PCl_3 exposure at 550°C for 10 min, and (d) O_3/HCl procedure and then PCl_3 exposure at 550°C for 10 min.

CHAPTER 6
SUMMARY

The effect of various cleaning techniques on III-nitride surfaces was investigated. Using only ex-situ cleaning methods, the lowest oxygen impurity levels on AlN and GaN surfaces were achieved after HF and HCl based treatments, while UV/O_3 cleaning was very effective for removing carbon. Further removal of the O and, for AlN, carbon as well, could be acieved after in-situ thermal cleaning with a H_2/N_2 plasma. Ex-situ acid and UV/O_3 cleaning followed by a PCl_3 treatment was the most effective at reducing C and O from the GaN surface. The AlN/GaN MIS diode treated with HCl/O_3 followed by PCl_3 exposure at 300°C showed the best I-V characteristics due to the decrease of the surface impurities or defects from the GaN surface and the better quality of the AlN layer growth after the treatment.

Rapid thermal annealing at temperatures $\geq 900^{\circ}C$ in a N_2 ambient degraded the GaN surface and this degradation affected the electrical properties of GaN Schottky dodes. The increase of surface carrier concentration after high temperature annealing due to the preferential loss of nitrogen from the GaN increased the reverse leakage current of the Schottky diodes. Some small recovery of breakdown vlotage was achieved due to the removal of the thermally damaged surface layer after PCl_3 chemical beam treatment.

In conclusion, even though complete removal of the surface C and O could not be achieved due to the very strong bonding of the C and O with III-nitride materials, the results of this study show the lowest C and O impurity level yet reported. It is likely that complete avoidance of exposure to air will be needed in order to avoid contamination at the GaN/dielectric interface in MOS devices. This will necessitate the use of multichamber deposition/processing systems to achieve the required material and interfacial quality.

LIST OF REFERENCES

1. S. Nakamura in *GaN and Related Materials*, edited by S. J. Pearton (Gordon and Breach Science Publishers, NY, 1997), P.471-507.

2. S. C. Binari and H. B. Dietrich in *GaN and Related Materials*, edited by S. J. Pearton (Gordon and Breach Science Publishers, NY, 1997), P.509-534.

3. H. Amano, N Sawaki, I. Akasaki and Y. Toyada, Appl. Phys. Lett. 48, 353 (1986).

4. M. E. Lin, B. Sverdlov, G. L. Zhou and H. Morkoç, Appl. Phys. Lett. 62, 3479 (1993).

5. I. Akasaki, H. Amano, M. Kito and K. Hiramatsu, J. Lumin. 48/49, 666 (1991).

6. S. Nakamura, M. Seno and T. Mukai, Jpn. J. Appl. Phys. 30, L1708 (1991).

7. C. Y. Hwang, Y. Li, M. J. Schurman, W. E. Mayo, Y. Lu and R. A. Stall, Mat. Res. Soc. Symp. Proc. 395, 521 (1996).

8. H. Kroemer, in *Molecular Beam Epitaxy and Heterostructures*, edited by L. L. Chang and K. Ploog, NATO ASI series E, No. 87 (1985).

9. J. L. Lee, M. Weber, J. K. Kim, J. W. Lee, Y. J. Park, T. Kim and K. Lynn, Appl. Phys. Lett. 74, 2289 (1999).

10. R. A. Logan and C. D. Thurmond, J. Electrochem. Soc. 119, 1727 (1992).

11. N. Y. Li, Y. M. Hsin, P. M. Asbeck and C. W. Tu, J. Crystal Growth 175/176, 387 (1997).

12. M. A. Jaso and G. S. Oehrlein, J. Vac. Sci. Technol. A6, 1397 (1988).

13. G. E. Potter, G. H. Morrison, P. K. Charvat and A. L. Ruoff, J. Vac. Sci. Technol. B10, 2398 (1992).

14. J. S. Foresi and T. D. Moustakas, Appl. Phys. Lett. 62, 2859 (1993).

15. V. M. Bermudez, T. M. Jung, K. Doverspike and A. E. Wickenden, J. Appl. Phys. 79, 110 (1996).

16. J. D. Guo, M. S. Feng, R. J. Guo, F. M. Pan and C. Y. Chang, Appl. Phys. Lett. 67, 2657 (1995).

17. J. Sun, K. A. Rickert, J. M. Redwing, A. B. Ellis, F. J. Himpsel and T. F. Kuech, Appl. Phys. Lett. 76, 415 (2000).

18. J. K. Kim, J. L. Lee, J. W. Lee, H. E. Shin, Y. J. Park, and T. I. Kim, Appl. Phys Lett, 73, 2953 (1998).

19. K. Hattori and Y. Izumi, J. Appl. Phys. 53, 6906 (1982).

20. P. Viktorovitch, M. Gendry, S. K. Krawczk, F. Krafft, P. Abraham, A. Bekkaoui, and Y. Monteil, Appl. Phys. Lett. 58, 2387 (1991).

21. E. K. Kim, H. Y. Cho, Y. Kim, H. S. Kim, M. S. Kim, and S. K. Min, Appl. Phys. Lett. 58, 2405 (1991).

22. T. Niwa, N. Furuhata, and T. Maeda, J. Crystal Growth, 175/176, 441 (1997).

23. T. M. Burke, M. A. Quierin, M. P. Grimshaw, D. A. Ritchie, and M. Pepper, J. Vac. Sci. Technol. B15, 325 (1997).

24. H. Kunzel, J. Bottcher, A Hase, H. J. Hensel, G. Urmann, and A. Paraskevopoulos, J. Crystal Growth, 175/176, 411 (1997).

25. A. Johnson, G. Williams, A. Pidduck, C. Whitehouse, T. Martin, C. Elliot, and T. Ashley, 7th Int. Conf. on *Narrow GaP Semiconductors* (1995).

26. D. S. L. Mui, T. A. Strand, B. J. Thibeault. L. A. Coldren, P. M. Petroff, and E. L. Hu, Inst. Phys. Conf. Ser. 141, 69 (1995).

27. T. Kaneko, P. Smilauer, B. A. Joyce, T. Kawamura, and D. D. Vredensky, Phys. Rev. Lett. 74, 3289 (1995).

28. M. Ritz, T. Kaneko, and K. Eberl, Appl. Phys. Lett. 71, 695 (1997).

29. J. Zhang, O. P. Naji, P. Steans, P. Tejeddor, T.m Kaneko, T. S. Jones, and B. A. Joyce, J. Crystal Growth, 175/176, 1284 (1997).

30. W. T. Tsang, T. H. Chiu, and R. M. Kapre, Appl. Phys. Lett. 63, 3500 (1993).

31. T. H. Chiu, M. D. Williams, J. F. Ferguson, W. T. Tsang, and R. M. Kapre, Appl. Phys. Lett. 65, 448 (1994).

32. J. M. Ortion, Y. Cordier, J. Ch. Garcia, and C. Grattepain, J. Crystal Growth, 164, 97 (1996).

33. W. T. Tsang, R. Kapre, and P. F. Sciortino, Jr., J. Crystal Growth, 136, 42 (1994).

34. W. T. Tsang, R. Kapre, and P. F. Sciortino, Jr., Appl. Phys. Lett. 62, 2084 (1993).

35. H. Asahi, X. F. Liu, K. Inoue, D. Marx, K. Asami, K. Miki, and S. Gonda, J. Crystal Growth, 145, 668 (1994).

36. C. W. Tu, H. K. Dong, and N. Y. Li, J. Crystal Growth, 163, 187 (1996).

37. S. Yoshida and M. Sasaki, J. Crystal Growth, 164, 291 (1996).

38. N. Y. Li, Y. M. Hsin, P. M. Asbeck, and C. W. Tu, J. Crystal Growth, 175/176, 387 (1997).

39. N. Y. Li, Y. M. Hsin, W. G. Bi, P. M. Asbeck, and C. W. Tu, Appl. Phys. Lett. 70, 2589 (1997).

40. N. Y. Li, H. K. Dong, W. S. Wong, and C. W. Tu, J. Crystal Growth, 164, 112 (1996).

41. K. Yamamoto, H. Asahi, T. Hayashi, K. Asami, and S. Gonda, J. Crystal Growth, 164, 117 (1996).

42. T. J. Whitaker, T. Martin, A. D. Johnson, A. J. Pidduck, and J. P. Newey, J. Crystal Growth, 164, 125 (1996).

43. K. Yamamoto, H. Asahi, K. Miki, and S. Gonda, J. Crystal Growth, 173, 21 (1997).

44. A. Izumi and H. Matsumura, Appl. Phys. Lett. 71, 1371 (1997).

45. C. C. Tin, A. Gichuhi, M. J. Bozack, C. G. Shannon, and C. K. The, Mat. Res. Soc. Symp. Proc. 468, 475, (1997).

46. S. Gwo and H. Tokumoto, Appl. Phys. Lett. 71, 362 (1997).

47. P. Hill, D. I. Westwood, L. Haworth, J. Lu, and J. E. Macdonald, J. Vac. Sci. Technol. B155, 1133 (1997).

48. M. H. Kim, C. Sone, J. H. Yi, and E. Yoon, Appl. Phys. Lett. 71, 1228 (1997).

49. M. Seelmann-Eggebert, H. Zimmermann, and H. Obloh, Mat. Res. Soc. Symp. Proc. 468, 193 (1997).

50. H. Ishikawa, S. Kobayashi, Y. Koido, S. Yamasaki, S. Nagai, J. Umezaki and M. Koike, J. Appl. Phys. 81, 1315 (1997).

51. J. L. Lee, J. K. Kim, J. W. Lee, Y. J. Park and T. Kim, Solid-State Electron. 43, 435 (1999).

52. S. D. Wolter, B. P. Luther, D. L. Waltemyer, C. Önneby, S. E. Mohney and R. J. Molnar, Appl. Phys. Lett. 70, 2156 (1997).

53. N. J. Watkins, G. W. Wicks and Yongi Gao, Appl. Phys. Lett. 75, 2602 (1999).

54. Tosja K. Zywietz, Jörg Neugebauer and Matthias Scheffler, Appl. Phys. Lett. 74, 1695 (1999).

55. V. M. Bermudez, J. Appl. Phys. 80, 1190 (1996).

56. K. Prabhakaran, T. G. Anderson and K. Nozawa, Appl. Phys. Lett. 69, 3212 (1996).

57. N. V. Edwards, M. D. Bremser, T. W. Weeks, Jr., R. S. Kern, R. F. Davis and D. E. Aspens, Appl. Phys. Lett. 69, 2065 (1996).

58. L. L. Smith, S. W. King, R. J. Nemanich and R. F. Davis, J. Electron. Mater. 25, 805 (1996).

59. S. W. King, L. L. Smith, J. P. Barnaak, J. H. Ku, J. A. Christman, M. C. Benjamin, M. D. Bremser, R. J. Nemanich, and R. F. Davis, Mat. Res. Soc. Symp. Proc. 395, 739 (1996).

60. S. W. King, J. P. Barnak, M. D. Bremser, K. M. Tracy, C. Ronning, R. F. Davis and R. J. Nemanich, J. Appl. Phys. 84, 5248 (1998).

61. Y. Li, Y. Lu, H. Shen, M. Wraback, C. Y. Hwang, M. Schurman, W. Mayo, T. Salagai, and R. A. Stall, Mat. Res. Soc. Symp.Proc. 395, 369 (1996).

62. A. Y. Polyakov, M. Shin, S. J. Pearton, M. Skowronski, D. W. Gerve, and J. A. Freitas, Mat. Res. Soc. Symp. Proc. 423, 607 (1996).

63. H. M. Liao, R. N. S. Sodhi and T. W. Coyle, J. Vac. Sci. Technol. A11, 2681 (1993).

64. A. Bellosi, E. Landi and A. Tampieri, J. Mater. Res. 8, 565 (1993).

65. S. Kumar and T. L. Tansley, Jpn. J. Appl. Phys. 34, 4154 (1995).

66. P. S. Wang, S. G. Malghan, S. M. Hsu and T. N. Wittberg, J. Mater. Res. 10, 302 (1995).

67. V. Y. Fominski, O. I. Naoumenko, V. N. Nevolin, A. P. Alekhin, A. M. Markeev and L. A. Vyukov, Appl. Phys, Lett. 68, 2243 (1996).

68. J. C. Zolper, H. H. Tan, S. Williams, J. Zou, D. J. H. Cockayne, S. J. Pearton, M. H. Crawford and R. F. Karlicek, Jr., Appl. Phys. Lett. 70, 2729 (1997).

69. R. G. Wilson, J. M. Zavada, X. A. Cao, R. K. Singh, S. J. Pearton, H. J. Guo, S. J. Pennycook, M. Fu, J. A. Sekhar, V. Sacrvepalli, R. J. Shul, J. Han, D. J. Rieger, J. C. Zolper and C. R. Abernathy, J. Vac. Sci. Technol. A17, 1226 (1999).

70. H. H. Tan, J. S. Williams, J. Zou, D. J. H. Cockayne, S. J. Pearton, J. C. Zolper and R. A. Stall, Appl. Phys. Lett. 72, 1190 (1998).

71. X. A. Cao, C. R. Abernathy, R. K. Singh, S. J. Pearton, M. Fu, V. Scarvepalli, J. A. Sekhar, J. C. Zolper, D. J. Rieger, J. Han, T. J. Drummond, R. J. Shul and R. G. Wilson, Appl. Phys. Lett. 73, 229 (1998).

72. H. S. Venugopalan and S. E. Mohney, Appl. Phys. Lett, 73, 1242 (1998).

73. Q. Z. Liu, L. S. Yu, S. S. Lau, J. M. Redwing, N. R. Perkins and T. F. Kuech, Appl. Phys. Lett. 70, 1275 (1997).

74. J. K. Sheu, Y. K. Su, G. C. Chi, M. J. Jou and C. M. Chang, Appl. Phys. Lett. **72**, 3317 (1998).

75. C. W. Wang, J. Y. Liao, C. L. Chen, W. K. Lin, Y. K. Su and M. Yokoyama, J. Vac. Sci. Technol. B17, 1545 (1999).

76. Y. Koide, T. Maeda, T. Kawakami, S. Fujita, T. Vemura, N. Shibata and M. Murakami, J. of Electron. Mater. 28, 341 (1999).

77. J. K. Sheu, Y. K. Su, G. C. Chi, W. C. Chen, C. Y. Chen, C. N. Huang, J. M. Hong, Y. C. Yu, C. W. Wang and E. K. Lin, J. of Appl. Phys. 83, 3172 (1997).

78. X. A. Cao, S. J. Pearton, F. Ren, J. R. Lothian. Appl. Phys. Lett. 73, 942 (1998).

BIOGRAPHICAL SKETCH

Kang-Nyung Lee was born in Taegu, Korea, on December 12, 1965. He received a B.S. in Physics at Kyungpook National University in 1987. After serving in the Korean Army as an officer for three and half years, he worked at Samsung Electronics Company for two years.

He began studies at the University of Florida in August 1995, and received his M.S. degree in Materials Science and Engineering in May 1997. He completed his Ph.D. in semiconductor materials under the supervision of professor Cammy R. Abernathy. He begins his new professional career at Samsung Electronics.

I certify that I have read this study and that in my opinion it conforms to acceptable standards of scholarly presentation and is fully adequate, in scope and quality, as a dissertation for the degree of Doctor of Philosophy.

Cammy R Abernathy, Chair
Professor of Materials Science and
Engineering

I certify that I have read this study and that in my opinion it conforms to acceptable standards of scholarly presentation and is fully adequate, in scope and quality, as a dissertation for the degree of Doctor of Philosophy.

Stephen J. Pearton
Professor of Materials Science and
Engineering

I certify that I have read this study and that in my opinion it conforms to acceptable standards of scholarly presentation and is fully adequate, in scope and quality, as a dissertation for the degree of Doctor of Philosophy.

Stanley Bates

Stanley Bates
Associate Engineer of Materials Science
and Engineering

I certify that I have read this study and that in my opinion it conforms to acceptable standards of scholarly presentation and is fully adequate, in scope and quality, as a dissertation for the degree of Doctor of Philosophy.

Rajiv Singh
Professor of Materials Science and
Engineering

I certify that I have read this study and that in my opinion it conforms to acceptable standards of scholarly presentation and is fully adequate, in scope and quality, as a dissertation for the degree of Doctor of Philosophy.

Fred Sharifi

Fred Sharifi
Associate Professor of Physics

This dissertation was submitted to the Graduate Faculty of the College of Engineering and to the Graduate School and was accepted as partial fulfillment of the requirements for the degree of Doctor of Philosophy.

August, 2000

M. J. Ohanian
Dean, College of Engineering

Winfred M. Phillips
Dean, Graduate School